SIMULATION OF GROUND-WATER FLOW NEAR THE NUCLEAR-FUEL REPROCESSING FACILITY AT THE WESTERN NEW YORK NUCLEAR SERVICE CENTER, CATTARAUGUS COUNTY, NEW YORK

by Richard M. Yager

U.S. GEOLOGICAL SURVEY

Water-Resources Investigations Report 85-4308

Prepared in cooperation with the

U.S. NUCLEAR REGULATORY COMMISSION

Ithaca, New York

1987

UNITED STATES DEPARTMENT OF THE INTERIOR

DONALD PAUL HODEL, Secretary

GEOLOGICAL SURVEY

Dallas L. Peck, Director

For additional information
write to:

Subdistrict Chief
U.S. Geological Survey
521 W. Seneca Street
Ithaca, New York 14850
Telephone: (607) 272-8722

Copies of this report can
be purchased from:

U.S. Geological Survey
Books and Open-File Reports
Federal Center, Bldg. 41
Box 25425
Denver, Colorado 80225
Telephone: (303) 236-7476

CONTENTS

PLATE

(in pocket)

ILLUSTRATIONS

ILLUSTRATIONS (continued)

TABLES

CONVERSION FACTORS AND ABBREVIATIONS

Conversion factors for the terms used in this report are given for readers who prefer to use inch-pound units rather than International System (SI) units.

Multiply SI unit	By	To obtain inch-pound units
	Length	
millimeter (mm)	0.03937	inch (in)
meter (m)	3.281	foot (ft)
kilometer (km)	0.6214	mile (mi)
centimeter (cm)	0.3937	inch (in)
	Area	
square meter (m^2)	10.76	square foot (ft^2)
	1.196	square yard (yd^2)
	0.0002471	acre
hectare (ha)	2.471	acre
square kilometer (km^2)	0.3861	square mile (mi^2)
	Volume	
cubic meter (m^3)	35.31	cubic foot (ft^3)
	1.307	cubic yard (yd^3)
	0.0008107	acre-foot (acre-ft)
	264.2	gallon (gal)
liter (L)	1.0577	quart (qt)
	Flow	
liter per second (L/s)	0.03531	cubic foot per second (ft^3/s)
cubic meter per second (m^3/s)	35.31	cubic foot per second (ft^3/s)
cubic meter per day (m^3/d)	0.0004086	cubic foot per second (ft^3/s)
	Hydraulic Units	
meter per day (m/d)	3.281	feet per day (ft/d)
	Temperature	
degree Celsius (°C)	°F = (9/5 °C) +32	degree Fahrenheit (°F)
	Other Abbreviation	
picocurie per milliliter	(pCi/mL)	

National Geodetic Vertical Datum of 1929 (NGVD of 1929): A geodetic datum derived from a general adjustment of the first-order level nets of both the United States and Canads, formerly called "Mean Sea Level."

Simulation of Ground-Water Flow Near the Nuclear-Fuel Reprocessing Facility at the Western New York Nuclear Service Center, Cattaraugus County, New York

By Richard M. Yager

ABSTRACT

A two-dimensional finite-difference model was developed to simulate ground-water flow in a surficial sand and gravel deposit underlying the nuclear-fuel reprocessing facility at Western New York Nuclear Service Center near West Valley, N.Y. The sand and gravel deposit overlies a till plateau that abuts an upland area of siltstone and shale on its west side, and is bounded on the other three sides by deeply incised stream channels that drain to Buttermilk Creek, a tributary to Cattaraugus Creek. Radioactive materials are stored within the reprocessing plant and are also buried within a till deposit at the facility. Tritiated water is stored in a lagoon system near the plant and released under permit to Franks Creek, a tributary to Buttermilk Creek.

Ground-water levels predicted by steady-state simulations closely matched those measured in 23 observation wells, with an average error of 0.5 meter. Simulated ground-water discharges to two stream channels and a subsurface drain were within 5 percent of recorded values. Steady-state simulations used an average annual recharge rate of 46 centimeters per year; predicted evapotranspiration loss from the ground was 20 centimeters per year. The lateral range in hydraulic conductivity obtained through model calibration was 0.6 to 10 meters per day. This range compares favorably with that calculated from slug tests at observation wells, although the mean value of 4.0 used in the model is considerably higher than the geometric mean value of 0.6 meter per day obtained from slug-test data.

Model simulations indicated that 33 percent of the ground water discharged from the sand and gravel unit (2.6 liters per second) is lost by evapotranspiration, 39 percent (3.0 liters per second) flows to seepage faces at the periphery of the plateau, 20 percent (1.6 liters per second) discharges to stream channels that drain a large wetland area near the center of the plateau, and the remaining 8 percent (0.6 liter per second) discharges to a subsurface french drain and to a wastewater-treatment system.

Ground-water levels computed by a transient-state simulation of an annual climatic cycle, including seasonal variation in recharge and evapotranspiration, closely matched water levels measured in eight observation wells. The difference between computed and observed ground-water levels could largely be explained by uncertainty in the timing and volume of recharge. The hydraulic conductance of seepage faces was varied seasonally to match measured base flows.

The model was used to delineate ground-water flow paths and to estimate travel times from potential sources of radioisotope contamination to discharge areas on the plateau. The model predicted that the subsurface drain and the

stream channel that drains the wetland would intercept most of the recharge originating near the reprocessing plant. A slug of water introduced at the main plant building would take approximately 500 days to reach either discharge point.

The model also was used to simulate ground-water flows of 1972, when tritium was detected in ground water discharging into the wetland. Flow paths predicted by the model do not support the assumption that leakage from wastewater lagoons 200 meters south of the wetland was the source of the tritium.

INTRODUCTION

The Western New York Nuclear Service Center is on a 1,350-ha tract of land acquired in 1961 by the New York State Office of Atomic Development near the village of West Valley in northern Cattaraugus County, about 48 km south of Buffalo (fig. 1). In 1963, the U.S. Atomic Energy Commission issued a permit to a private operator authorizing development of about 100 ha of the tract for construction of a nuclear-fuel reprocessing plant and its facilities. The facilities included a receiving and storage facility for irradiated fuel rods, an underground tank complex for storage of liquid high-level radioactive wastes generated by reprocessing, and a low-level radioactive-wastewater-treatment plant. The site also included two areas for shallow burial of solid radioactive wastes--a 4-ha area licensed by the State of New York for burial of commercial low-level radioactive wastes and a 2.9-ha area previously licensed by the U.S. Nuclear Regulatory Commission for burial of radioactive materials from the reprocessing plant, called the facility's disposal area. Locations of the facilities are shown in figure 2.

In 1982, the reprocessing plant was turned over to the U.S. Department of Energy (DOE), which contracted the operation of the facility to a private operator, West Valley Nuclear Services, Inc.

The aim of the DOE is to decommission the reprocessing facilities and to solidify the high-level liquid radioactive waste stored at the site for future disposal at a high-level-waste repository.

The U.S. Geological Survey conducted studies from 1975 through 1980 to evaluate the potential for radioisotope migration from the State-licensed burial ground. The studies were part of a national program to determine the principal factors that control the subsurface movement of radioisotopes. Complementary studies by the New York State Geological Survey were done to evaluate other processes of radioisotope migration from the burial ground (Prudic, 1986).

In 1980, the U.S. Geological Survey, under contract with the U.S. Nuclear Regulatory Commission, began a study to investigate the hydrogeology and ground-water flow near the reprocessing plant and its facilities. The reprocessing plant is on the 42-ha north plateau, which is separated from the burial ground and facility's disposal area by a deeply incised stream channel, Erdman Brook. A companion study, also begun in 1980, examined the hydrogeology and ground-water flow in the facility's disposal area (Bergeron and Bugliosi, in press).

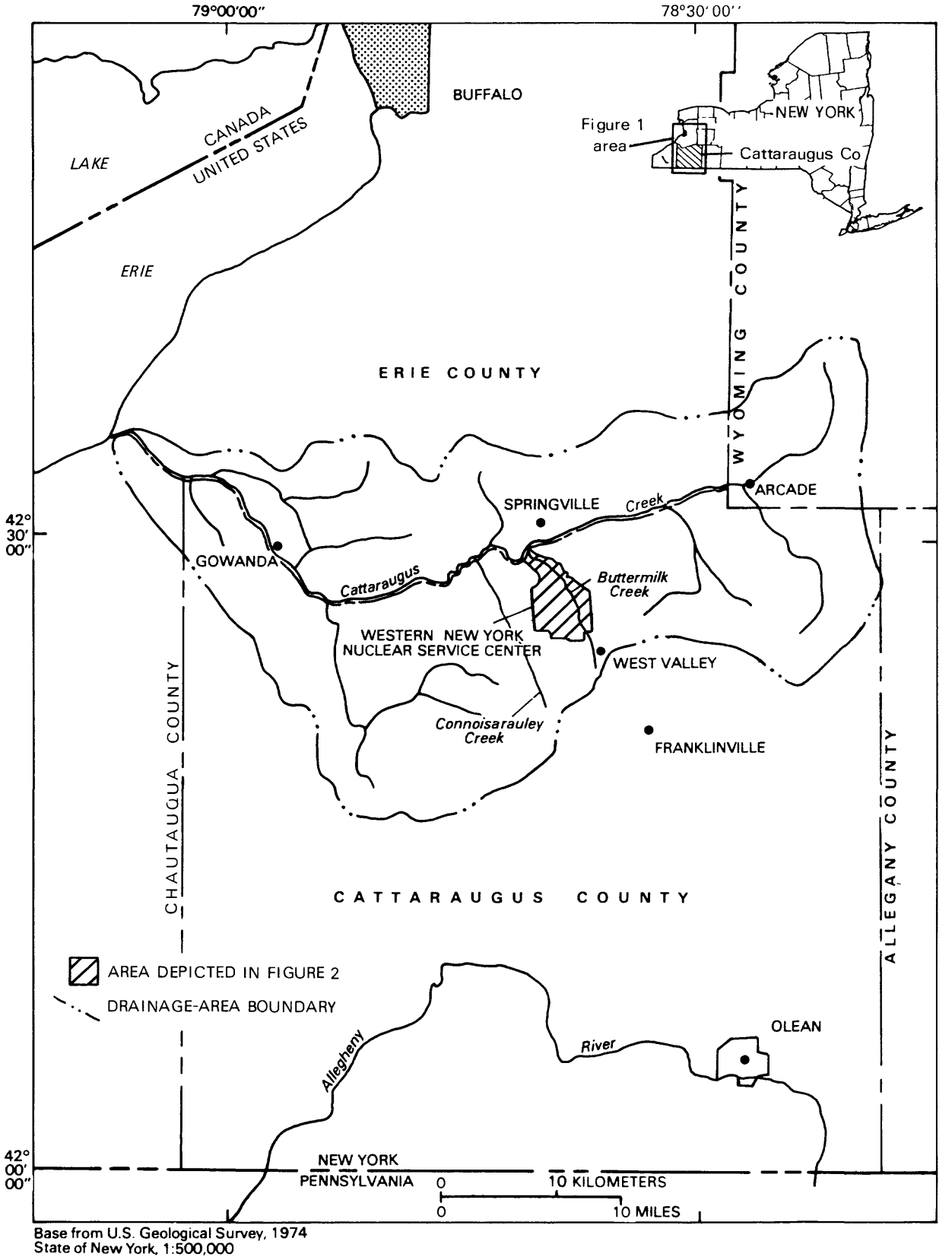

Figure 1.--Location of study area within Cattaraugus Creek drainage basin.

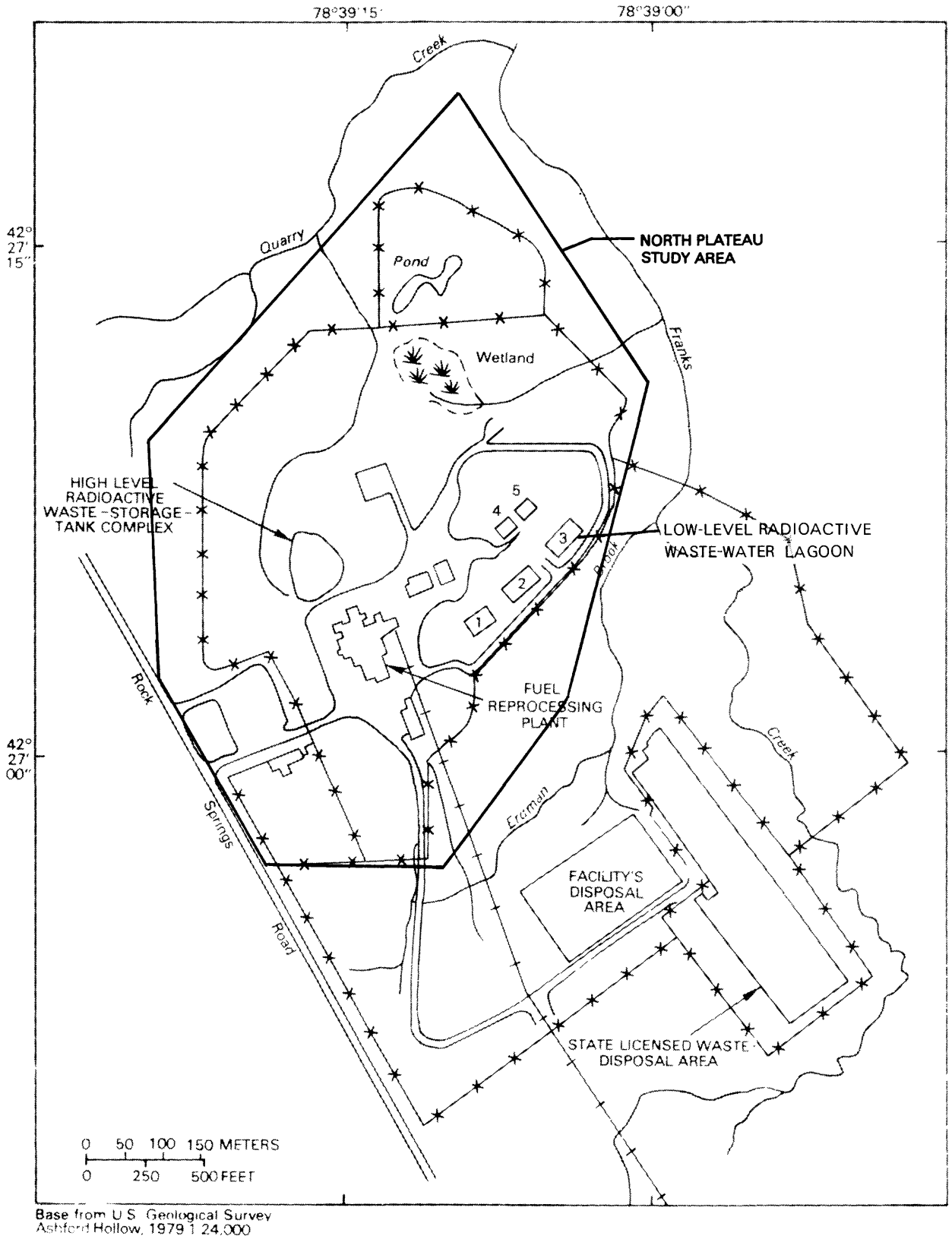

Figure 2.--Location of nuclear-fuel-reprocessing plant and related waste facilities. (General location is shown in fig. 1.)

Purpose and Scope

This report describes (1) hydrogeologic conditions and ground-water flow near the reprocessing plant and its facilities on the north plateau, (2) the reprocessing-plant facilities and the migration of radioisotopes in the area, (3) ground-water flow patterns on the north plateau within the surficial sand and gravel deposit, (4) the development and calibration of a two-dimensional finite-difference model used to simulate steady- and transient-state flow within the surficial material, and (5) the application of the model to analyze past tritium migration and to predict flow paths and velocities of ground water from two potential sources of tritium detected in 1972.

Acknowledgments

The author thanks the staff of the West Valley Nuclear Service Center for cooperation and assistance in recording water levels and supplying data on the plant operation and construction. Thanks are also extended to T. S. Steenhuis, professor of Agricultural Engineering at Cornell University, for assistance in developing a model to simulate soil-moisture content that was used in calibrating values of ground-water recharge for the flow model.

SITE DESCRIPTION AND HISTORY

The Western New York Nuclear Service Center was operated as a nuclear-fuel reprocessing facility during 1966-72, during which time it received spent fuel-rod assemblies from nuclear reactors and processed the fuel elements to recover uranium and plutonium. Until 1975 the facility continued to receive fuel-rod assemblies. In 1985 the site contained spent fuel-rod assemblies that had not been reprocessed, high-level radioactive liquid wastes generated by the recovery process, and a variety of low-level radioactive solid wastes generated by the reprocessing facility and received from offsite commercial installations.

Reprocessing-Plant Facilities

The reprocessing plant consists of many facilities used in the recovery process (fig. 3). Three of these--the fuel-receiving and storage area, the high-level radioactive liquid-waste-tank complex, and the low-level radioactive wastewater-treatment system (fig. 3)--contain radioactive liquid waste and wastewater and are of concern as a potential source of radioisotope migration to ground water.

The fuel-receiving and storage area, which occupies the east part of the main plant, was the point of entry for fuel-rod assemblies received at the site. The area includes a fuel-storage pool in which the fuel-rod assemblies were submerged in demineralized water that is kept between 27° and 32°C. The fuel-storage pool is constructed of concrete lined with carbaloy paint and contains 3.0×10^6 liters of water.

The high-level liquid-waste-tank complex (fig. 3) serves as a temporary repository for waste solutions from the recovery process used in the reprocessing facility. The tank complex consists of two underground concrete vaults,

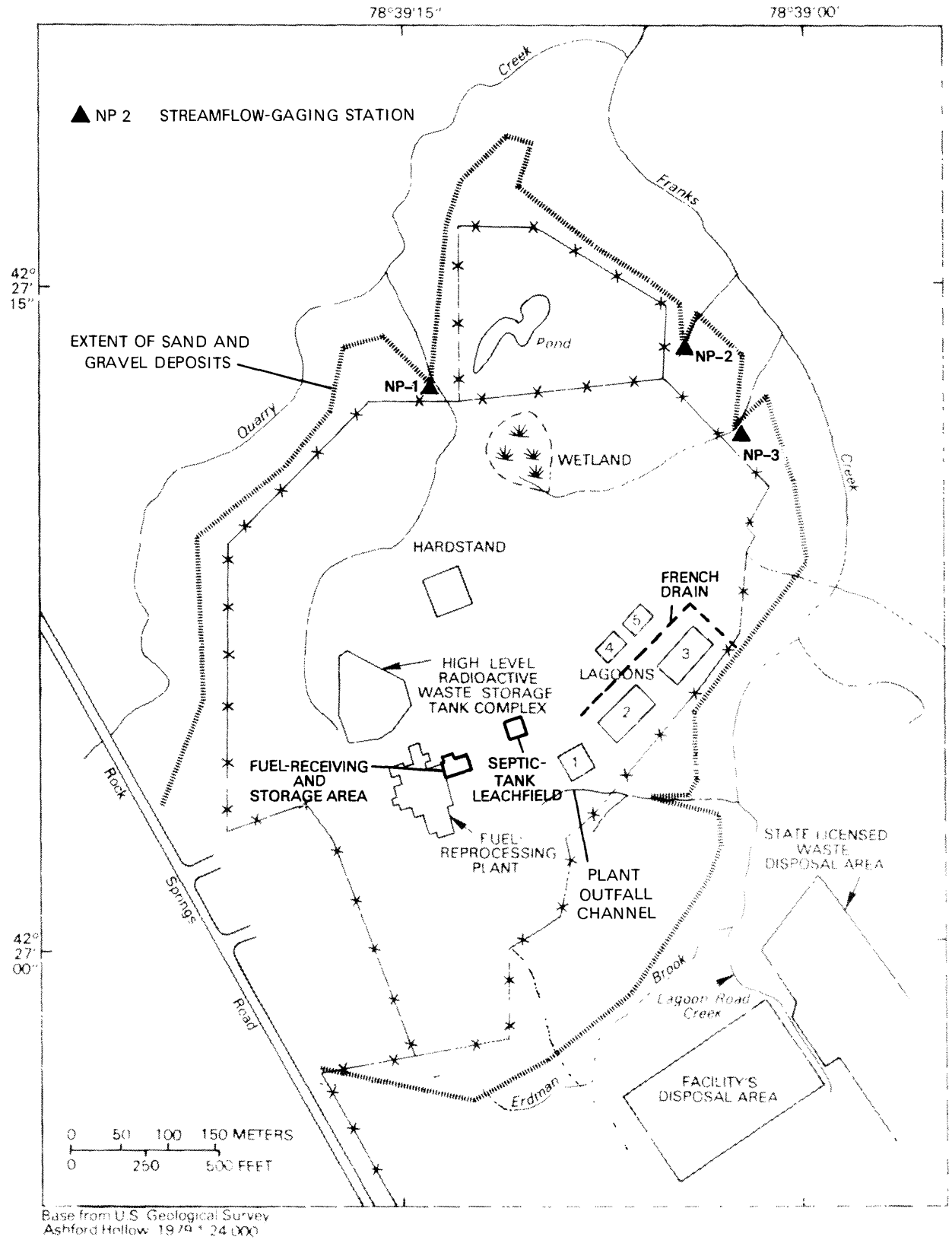

Figure 3.--Location of reprocessing-plant facilities and repositories of radioactive liquid waste and wastewater on north plateau.

each of which encases two cylindrical stainless-steel tanks. The entire complex is backfilled with 8 m of silty clay till. An external hydraulic pressure is maintained by a water-injection system in a 1.2-m layer of pea gravel beneath the tank complex to prevent leakage from the concrete vaults. Nearly 98 percent of the 2.2×10^6 liters of liquid waste is stored in one tank. Vapor ventilated from the concrete vault is regularly monitored for radioactive leakage from the storage tanks.

The low-level wastewater-treatment system, 100 m east of the main plant, was designed to remove radioisotopes from wastewater generated by reprocessing operations and to release the treated water to surface water at a controlled rate. Since the shutdown of the reprocessing plant in 1972, the system has treated 20 to 60 x 10^6 m/yr of wastewater from (1) precipitation that had infiltrated into the State-licensed burial ground, (2) condensate from the cooling system of the fuel-storage pool, and (3) rinse water from decontamination activities.

The facility originally included five lagoons for storage of processed and unprocessed wastewater. A schematic diagram of the low-level-radioactive wastewater system showing the relative sizes of the lagoons and direction of flow is given in figure 4. The wastewater entered the system through lagoon 1, passed to lagoon 2 for temporary storage, and was periodically withdrawn from lagoon 2 and back through lagoon 1 for treatment. The treated water was pumped to lagoons 4 and 5 and then drained to lagoon 3, from which it was released to Erdman Brook (fig. 2). In 1984 lagoon 1 was backfilled, and wastewater was discharged directly into lagoon 2.

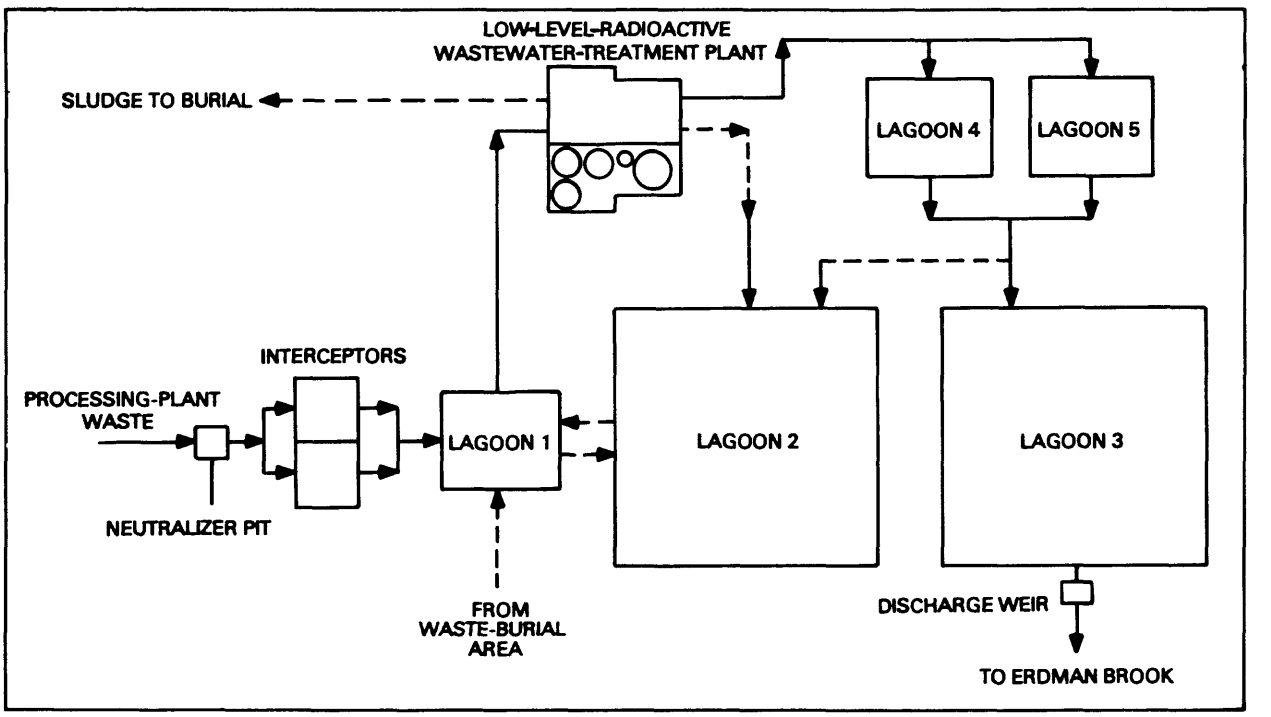

Figure 4.--Flow diagram of low-level radioactive wastewater-treatment system. (Modified from U.S. Department of Energy, 1979.)

A subsurface (french) drain was installed on the north and west sides of lagoons 2 and 3 to intercept and reduce ground-water seepage into them. The drain consists of a 15-cm-diameter perforated pipe buried about 3 m below land surface. The drain discharges to Erdman Brook east of lagoon 3. (See fig. 3.)

Migration of Radioisotopes

Migration of radioisotopes from the reprocessing facility has been documented by radiation surveys of the land surface and soil samples (L. Roberts, West Valley Nuclear Services Co., written commun., 1984). Gamma-radiation surveys on the 42-ha north plateau detected surface radiation 10 to 100 times the background level recorded offsite. The shape of the radiation field indicated that the probable source of the surface contamination was particulate fallout from the ventilation stack of the main plant building. A soil-sampling survey showed that surface deposits of particulate radioactive materials were retained in the upper 25 cm of soil (L. Roberts, written commun., 1984). This indicates that most radioactive-decay products generated by the reprocessing facility adsorb readily to clay surfaces in subsurface materials and do not tend to migrate with ground water.

Tritium is the most mobile radioisotope found in ground water and is the only one detected in ground-water samples from the north plateau (L. Roberts, written commun., 1984). Concentrations of tritium at selected locations are listed in table 1. Above-background concentrations were detected in 1972 in ground water that discharged to the wetland and the french drain. In response to this discovery, several shallow wells were installed near the main plant to determine the tritium source. Analysis of water samples from these wells indicated that the low-level wastewater-treatment system was the probable source of tritium in ground water. Fallout from the ventilation stack was less likely to contribute tritium to ground water because the tritium emerged from the stack in the form of water vapor and would thus be carried away from the plateau by air currents.

Table 1.--Tritium concentration of liquid waste and wastewater in reprocessing-plant facilities, 1979.

Location	Concentration (pCi/mL)
Fuel-storage pool	600
High-level liquid-waste tank	22,000
Lagoon 1	1,500-100,000
Unaffected areas (background levels)	2

The concentrations of tritium in ground water that discharged to the wetland and the french drain during 1973-81 are plotted in figure 5; those in wells near the lagoons in 1974 and 1978 are shown in figures 6A and 6B, respectively. The abrupt rise in tritium concentration at the french drain in 1976 is attributed to overflow from lagoon 3. The concentrations declined as the lagoon was emptied but remained above the background concentration in samples collected offsite. The source of this continuing radioactivity was assumed to be lagoon 1, which was unlined and hydraulically connected to ground water. Lagoon 1 was backfilled in 1984 and is no longer part of the treatment system.

The concentrations of tritium in ground water at wells near the lagoons in June 1974 are shown in figure 6A. Tritium concentrations at most wells declined after lagoons 4 and 5 were sealed with rubber liners in October 1974 and reprocessing activities ceased; the concentrations at the same wells in 1978 are shown in figure 6B. Tritium concentrations were generally highest near lagoon 1, but relatively high tritium concentrations were also found in wells north of the reprocessing plant. The tritium in ground water north of the plant could have originated from contamination that has occurred beneath the main plant building (New York State Department of Environmental Conservation, 1975, p. 12). Other possible sources could be tritium released from the ventilation stack during cold weather and carried to the land surface by snowfall, or leaking containers of tritiated water that may have been stored on the hardstand, a small paved area north of the reprocessing plant (fig. 3).

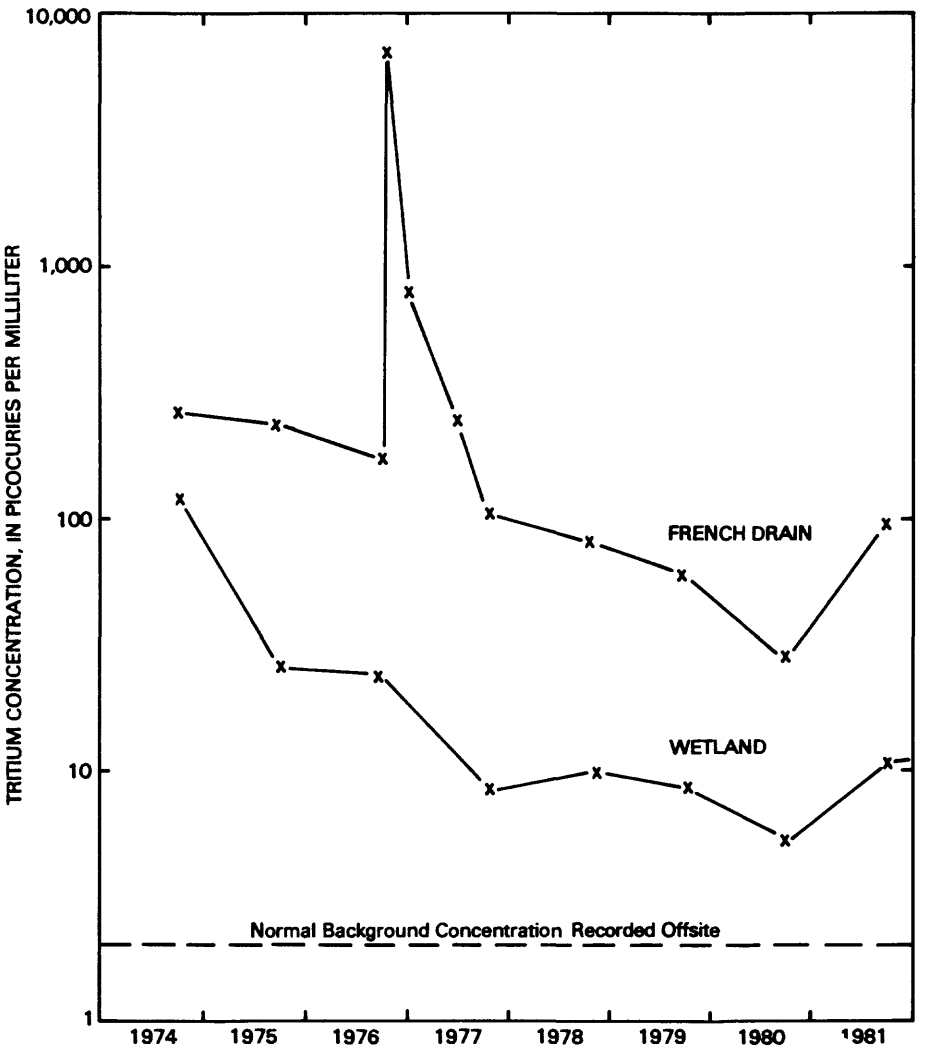

Figure 5.--Tritium concentrations in ground water that discharged to the wetland and french drain, 1974-81.

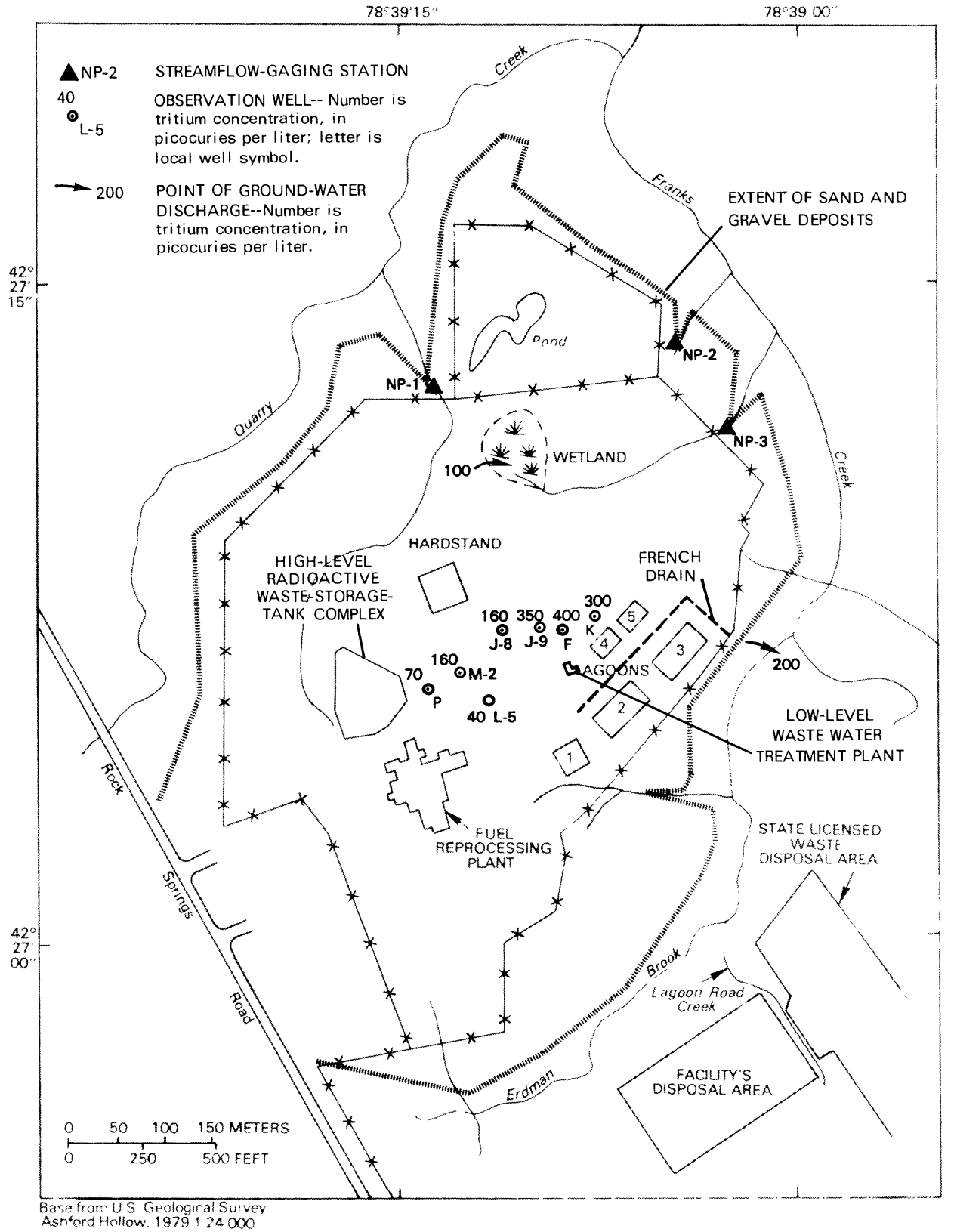

Figure 6A.--Tritium concentrations in ground-water samples collected from north plateau in 1974, before lagoons were sealed. (Location is shown in fig. 2.)

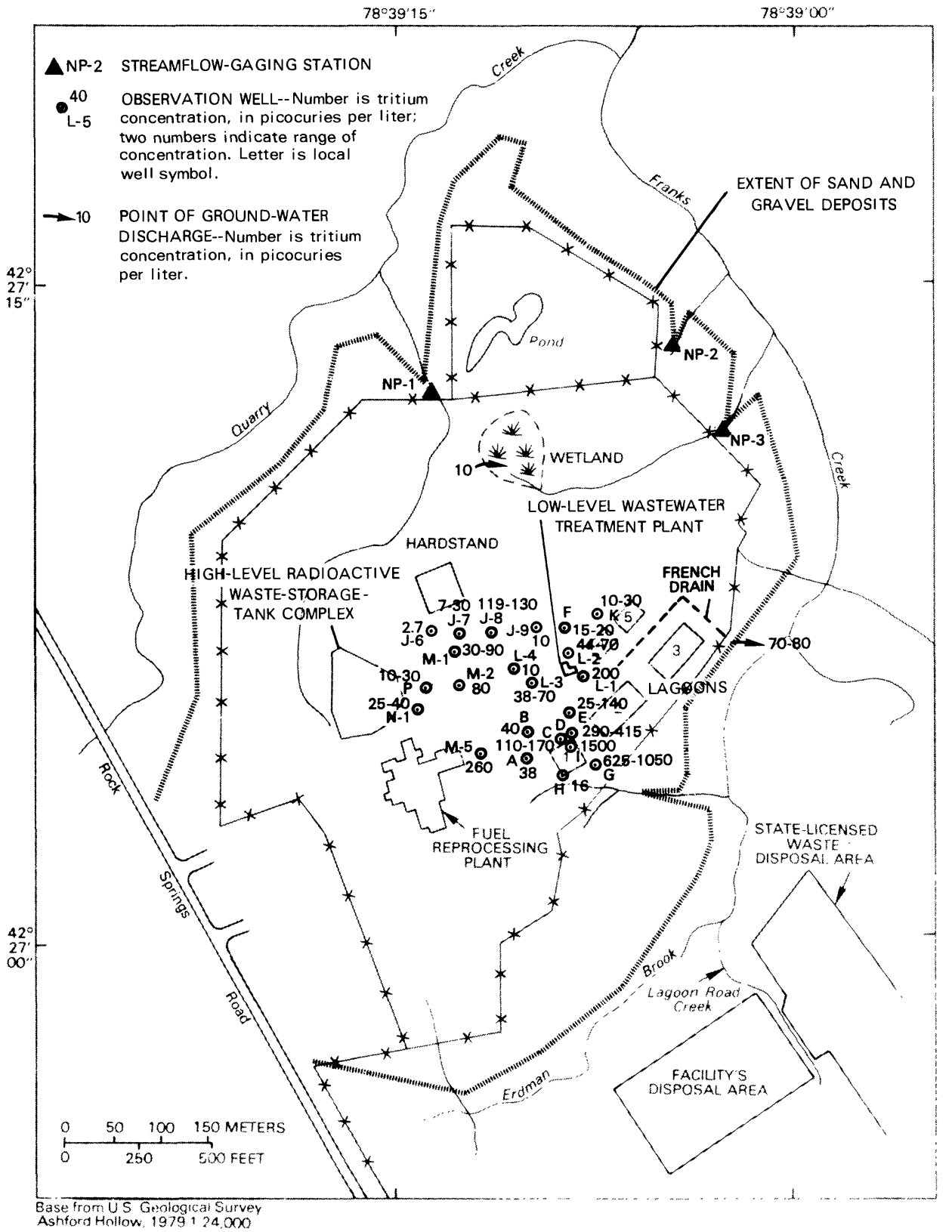

Figure 6B.--Tritium concentrations of ground-water samples collected from north plateau in 1978, after lagoons 4 and 5 had been sealed for 4 years. (Location is shown in fig. 2.)

HYDROGEOLOGIC SETTING

Drainage

The study area lies along the west side of the Buttermilk Creek valley (fig. 1). Buttermilk Creek flows northwestward along the east side of the site to Cattaraugus Creek near Springville, about 3 km north of the site. Cattaraugus Creek drains to Lake Erie.

Franks Creek, a major tributary to Buttermilk Creek, drains the entire site. It has a drainage area of 6.35 km^2 and borders the north plateau on the east (fig. 2). Two of its smaller tributaries, Quarry Creek and Erdman Brook, border the north plateau on the northwest and southeast, respectively.

The north plateau is drained by three small unnamed tributary streams. The westernmost stream, with a gaging station designated North Plateau 1 (hereafter referred to as NP1), drains the west side of the plateau and is tributary to Quarry Creek (fig. 3). The gaged drainage area is 10.4 ha. The second stream is upstream from gaging station NP3 (fig. 3) and is intermittent; it drains 9.8 ha and is tributary to Franks Creek. This channel receives flow from the center of the plateau, including the wetland and most of the reprocessing facilites. The third stream drains a 1.8-ha area upstream from the partial-record station designated NP2 (fig. 3); it also is intermittent and is tributary to Franks Creek. This channel was the outlet of the wetland, which now drains past station NP3 as a result of topographic modifications during site development. Most of the water discharged from the easternmost 7.5 ha of the plateau is from the main plant's steam-condensation system combined with overflow from the plant's water-supply system. The french-drain system that surrounds Lagoons 2 and 3 (fig. 6B) also discharges perennially to Erdman Brook.

Climate

Mean annual temperature at the site is 7.2°C. The warmest month is July, with a mean temperature of 19.6°C; the coldest month is February, with a mean temperature of -5.7°C. Mean annual precipitation is about 100 cm; this amount is distributed fairly evenly throughout the year.

Monthly precipitation and estimated potential evapotranspiration (fig. 7) were used to estimate total recharge to ground water on the north plateau from October 1982 through September 1983. Approximately 13 percent of the precipitation flows over the surface of the north plateau as storm runoff (Kappel and Harding, 1987). Estimated potential evapotranspiration was calculated by a method based on the Penman equation (Steenhuis and others, 1983). The maximum and minimum daily temperature values used were those recorded at weather stations in Gowanda, Franklinville, and Arcade (fig. 1); percent cloud cover and average wind speed were recorded at the Buffalo Airport. Annual precipitation for the 12-month period was 92 cm, and the potential evapotranspiration was estimated to be 90 cm. Evapotranspiration from native grasses alone would be 68 cm, assuming a consumptive-use coefficient of 0.75 (Gray, 1970, p. 354).

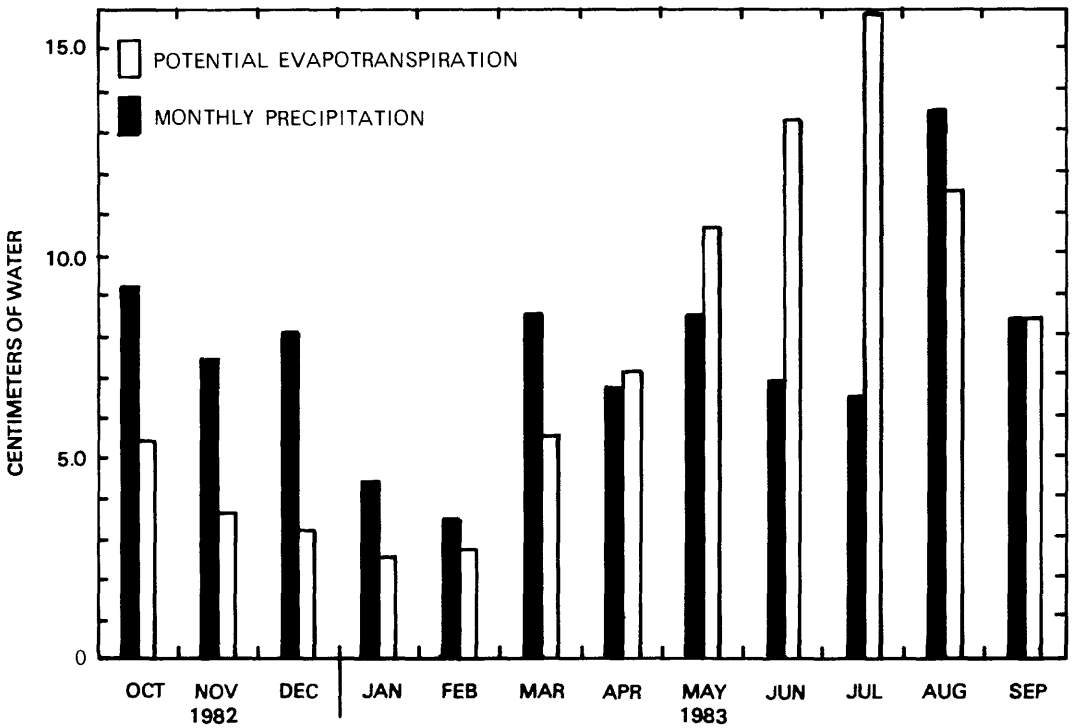

Figure 7.--Monthly precipitation and potential evapotranspiration on the north plateau, October 1982 through September 1983.

Geology

The Western New York Nuclear Service Center site is in the glaciated section of the Appalachian Plateau in western New York State, an area characterized by deeply dissected glacial drift overlying shale and sandstone. The north plateau consists of a sequence of glacial and postglacial deposits that reflect successive periods of glaciation as described by LaFleur (1979). Geologic data were available from 11 test borings completed by the U.S. Geological Survey and 87 test borings and pits completed by other investigators. Logs of these borings are presented in Bergeron (1985). Locations of wells and test borings in the study area are shown on plate 1.

The plateau is covered by a layer of silty sand and gravel deposited as an alluvial fan at the edge of a postglacial lake that formed in the Buttermilk Creek valley during the recession of the last ice margin. This deposit overlies a sequence of till deposits that probably correspond to three advances of the ice margin into the Buttermilk Creek valley. The till deposits are separated by lacustrine silt and sand, and by alluvial sand and gravel deposited during the recession of each ice margin. This sequence is depicted in section A-A' in figure 8A (lines of section are shown in pl. 1).

The surficial sand and gravel deposit and the underlying glacial deposits have been eroded by Buttermilk Creek and its tributaries to a maximum depth of 40 m. Today, the plateau area is bordered on three sides by gullies. The shale bedrock is at land surface at the southwest edge of the plateau, where it is in contact with the surficial sand and gravel.

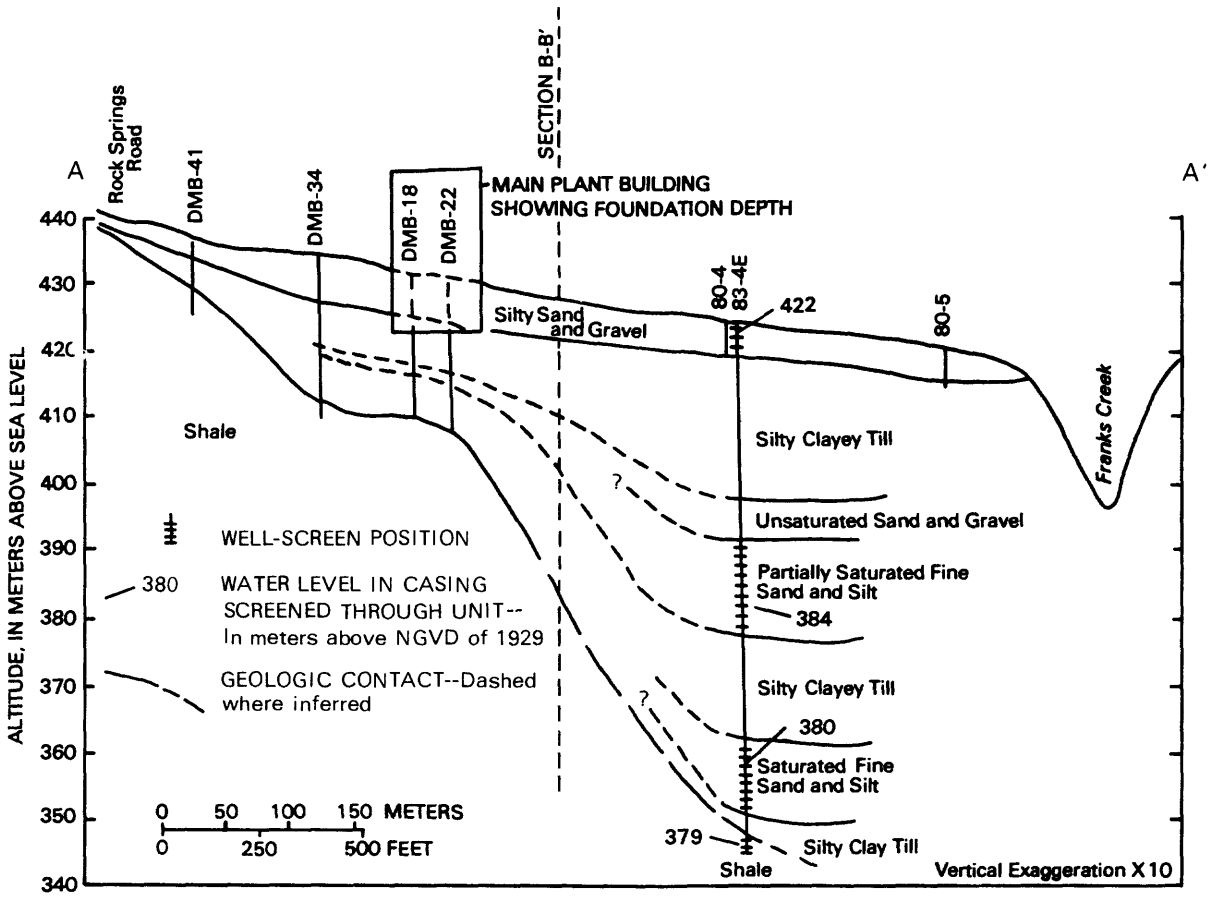

Figure 8A.--General hydrogeologic section A-A' showing major lithologic units from the main reprocessing-plant area to Franks Creek and water levels measured in well 82-4E, July 1983. Location of wells and line of section are shown on plate 1. (Modified from Bergeron and others, 1987.)

Water-Bearing Units

Unconfined ground water saturates the lower part of the surficial sand and gravel where it immediately overlies the till. The general position of the water table and the direction of ground-water flow through the surficial sand and gravel along section B-B' are shown in figure 8B. The saturated thickness of the sand and gravel on May 10, 1983 is depicted on the map shown in figure 9 (p. 16).

The sand and gravel deposit varies in composition but averages 55 percent gravel, 20 percent sand, and 25 percent silt. It is mostly silty gravel with some sand and has a high hydraulic conductivity. Where the deposit is thick, it contains thin layers of gravelly silt of lower hydraulic conductivity. The sand and gravel on the lower (central) part of the north plateau near well 80-6 (pl. 1) is covered with 3 m of silty till that was applied as fill to cover a wetland area.

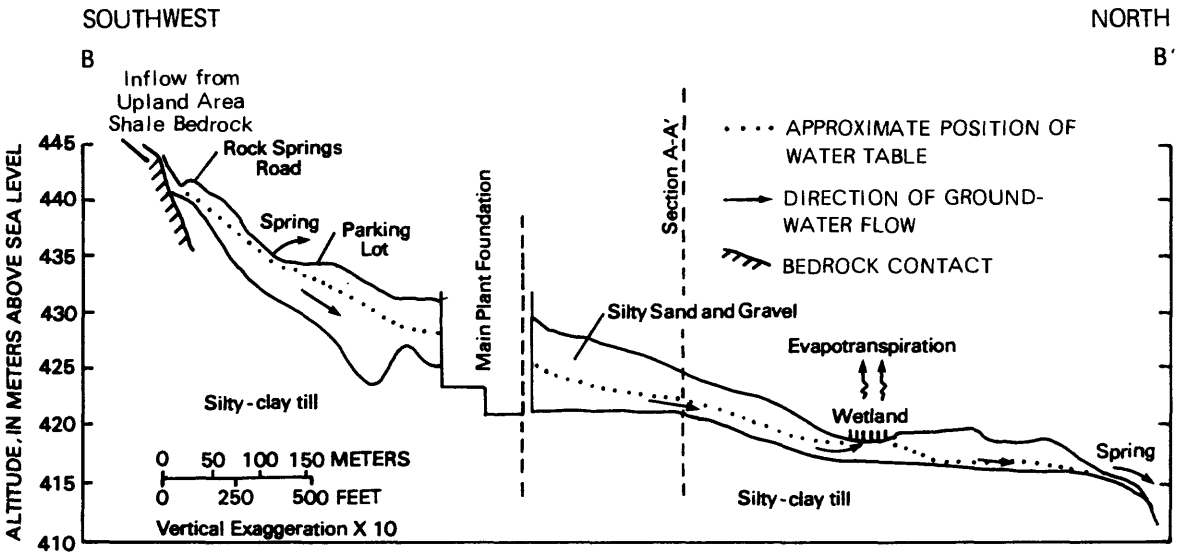

Figure 8B.--Generalized hydrogeologic section B-B' from shale uplands to Franks Creek showing water-table altitude on the north plateau, May 10, 1983. (Line of section is shown on pl. 1.)

The only other major water-bearing unit on the north plateau is the upper 1 m of the shale bedrock. The upper part of the bedrock is fractured and yields approximately 0.6 L/s to borehole 83-4E (fig. 8A).

Although largely saturated, the till deposits underlying the surficial sand and gravel do not transmit significant quantities of ground water because of their low hydraulic conductivity. The recessional deposits of sand and silt that separate the till deposits are also partly saturated and yield some water to borehole 83-4E (fig. 8A). However, the thickness and low hydraulic conductivity of the till deposits restricts ground-water flow to the lower recessional deposits and bedrock units. Thus, the surficial sand and gravel unit is the most significant aquifer near the reprocessing-plant facilities.

HYDROLOGY OF THE SURFICIAL SAND AND GRAVEL

The following discussion is based on data collected from October 1981 through September 1983 and on the results of the ground-water flow model simulations discussed further on. During the data-collection period, ground-water levels were measured monthly in 25 observation wells finished in the surficial sand and gravel, and slug tests were done to obtain estimates of hydraulic conductivity for use in the model. Streamflow in the two intermittent-stream channels that drain the north plateau to Quarry and Franks Creek was recorded continuously at stations NP-1 and NP-3. Altitudes of springs and seepage faces along the periphery of the plateau were surveyed, and discharges from these areas were measured periodically.

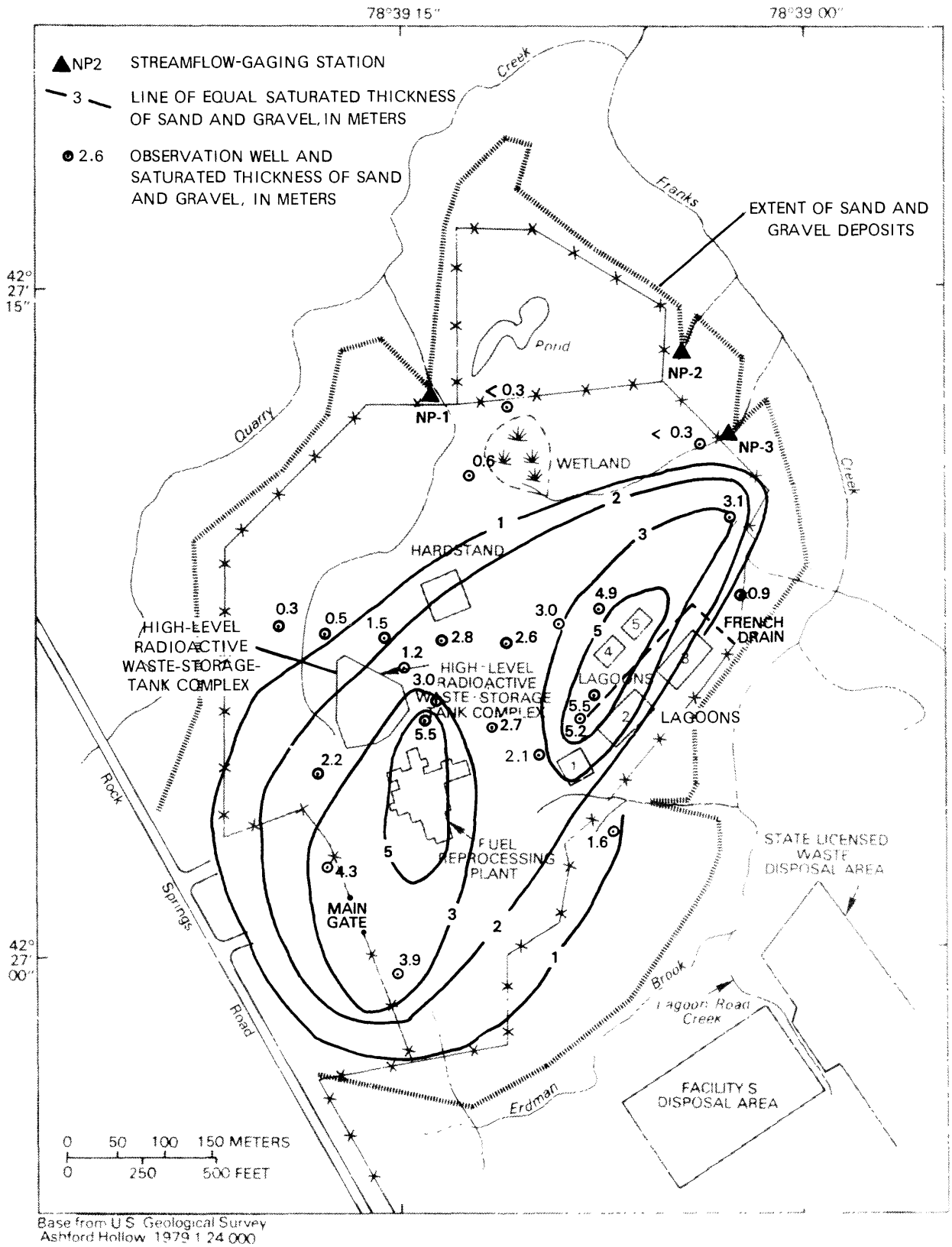

Figure 9.--Saturated thickness of surficial gravel on north plateau, May 10, 1983. (Modified from Bergeron and others, 1987.)

Flow Direction Under Undisturbed Conditions

Ground water in the surficial sand and gravel flows radially away from the apex of the alluvial fan at the upland (southern) boundary and northeastward toward stream channels bordering the plateau. Some of the water from the fractured bedrock along the upland boundary probably enters the sand and gravel deposit; the remainder moves northward within the bedrock. Ground-water flow through the sand and gravel is predominantly horizontal, and leakage into the underlying till is inconsequential. Discharge from the sand and gravel occurs by evapotranspiration and by seepage to intermittent-stream channels that drain the plateau and to springs and seepage faces above the contact between the gravel and till along the periphery of the plateau. The directions of ground-water flow through the sand and gravel, shown in figure 10, are based on ground-water levels recorded in May 1983 and the altitudes of springs.

Influence of Plant Facilities on Ground-Water Flow

The plant facilities indicated on figure 3 have altered the natural ground-water flow pattern by obstructing flow in some areas and providing preferential discharge points in others. The effects of these structures are discussed below.

High-Level Liquid-Waste-Tank Complex

The high-level liquid-waste-tank complex and the fuel-storage pool fully penetrate the surficial sand and gravel deposit and prevent the flow of ground water through these areas. The backfill that surrounds these structures is less permeable than the original materials, and this restricts ground-water flow.

Drainage Structures

Two drainage structures--the french drain adjacent to lagoons 2 and 3 and the ditch connecting the wetland to the stream channel above station NP-3 (fig. 9)--were installed to dewater parts of the north plateau. These stations receive most ground-water discharge, and ground water flows toward these areas. Flow at both stations is continuous through the year.

Wastewater Lagoons

The low-level waste-treatment system has influenced the ground-water flow system in the past by serving both as a source of recharge and a point of discharge. Lagoons 4 and 5 were built above land surface in 1971 and, although their bottoms were sealed with silty clay till, wastewater leaked to the surficial sand and gravel. In 1974 the lagoons were lined with a synthetic material to prevent further leakage. Lagoons 2 and 3 were both excavated into the till underlying the sand and gravel, yet wastewater can leak into the surficial deposits whenever the water level in the lagoons rises above the contact between the till and the gravel. Since such an incident in 1976, water levels have been controlled to prevent lateral leakage from the lagoons. The french drain has reduced seepage to lagoons 2 and 3, but seepage still occurs along the southwest face of lagoon 2.

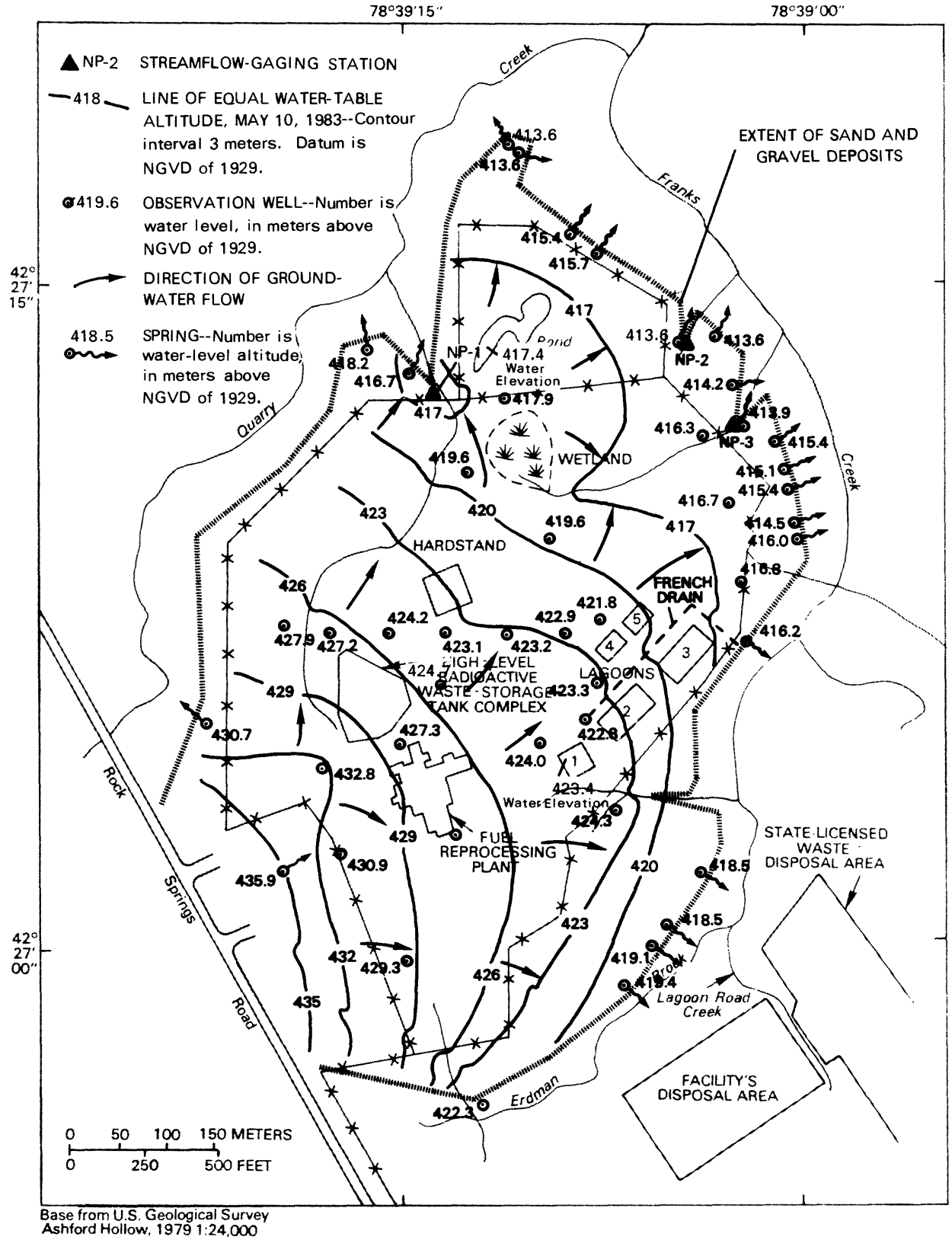

Figure 10.--Water-level altitude and direction of ground-water flow on the north plateau, May 10, 1983.

Before lagoon 1 was removed from the low-level waste-treatment system in 1984, it was hydraulically connected to ground water in the surficial sand and gravel, which allowed leakage both to and from the lagoon. Lagoon 1 accepted wastewater from the reprocessing facility and the burial grounds only periodically; most of the time, ground water seeped into lagoon 1 and flowed from there into lagoon 2. During periods in which wastewater was transferred into lagoon 1, the temporary increase in hydraulic head probably caused leakage from the lagoon into the ground water. The lagoon also caused a net loss of ground water through evaporation and overflow into lagoon 2 and thus represented a ground-water-discharge point.

Other Structures

Other structures that influence ground-water flow through the surficial sand and gravel are plant buildings and parking lots, which, together with the lagoons, drain to stream channels and have reduced by 17 percent the permeable area on the plateau through which rainfall can infiltrate and recharge the ground-water system. Potential sources of ground-water recharge include a septic-tank leach field attached to the maintenance shop, possible leaks from underground water lines northeast of the plant, and infiltration from the plant's outfall channel that crosses the sand and gravel near lagoon 1 (fig. 3). The outfall channel carries condensate and backwash from water filters and discharges to Erdman Brook east of lagoons 2 and 3. (See fig. 3.)

Water-Transmitting Properties of Sand and Gravel Deposit

Hydraulic conductivity of the sand and gravel was estimated from slug-test data and later modified during calibration of the flow model. The procedure for estimating hydraulic conductivity from slug-test data is explained in the appendix. The assumed lateral distribution of hydraulic conductivity is shown in figure 11. The range of values, 0.6 to 10.0 m/d, compares favorably with the range obtained from slug tests (see table 7, further on), although the average value of 5.0 m/d is significantly higher than the geometric mean of 0.6 m/d from slug-test results. This difference is probably due to errors in interpretation of the slug-test data, as discussed in the appendix.

Low hydraulic-conductivity values are associated with backfilled areas near the main plant building, the high-level liquid-waste complex, and the low-level waste-treatment facility. The low hydraulic conductivity in these areas causes a steeper hydraulic gradient west of the main plant than to the north (fig. 10). Areas of high hydraulic conductivity correspond to a buried stream channel on the surface of the till underlying the sand and gravel and produce the flatter gradient north of the plant. The channel may be an erosional feature that marks the location of a former stream channel cut into the surface of the till plateau. The resulting channel deposit would be composed of coarser material than that of the surrounding area. The location of the channel is shown in figure A-1 in the appendix.

The specific yield of the surficial sand and gravel was assumed to range from 0.10 to 0.25 in accordance with values reported in Todd (1980, p. 38). Lower values correspond to areas with a high silt content or to areas where a confining layer of silt and clay or fill overlies the deposit. Higher values were assumed to represent areas of well-sorted sand and gravel.

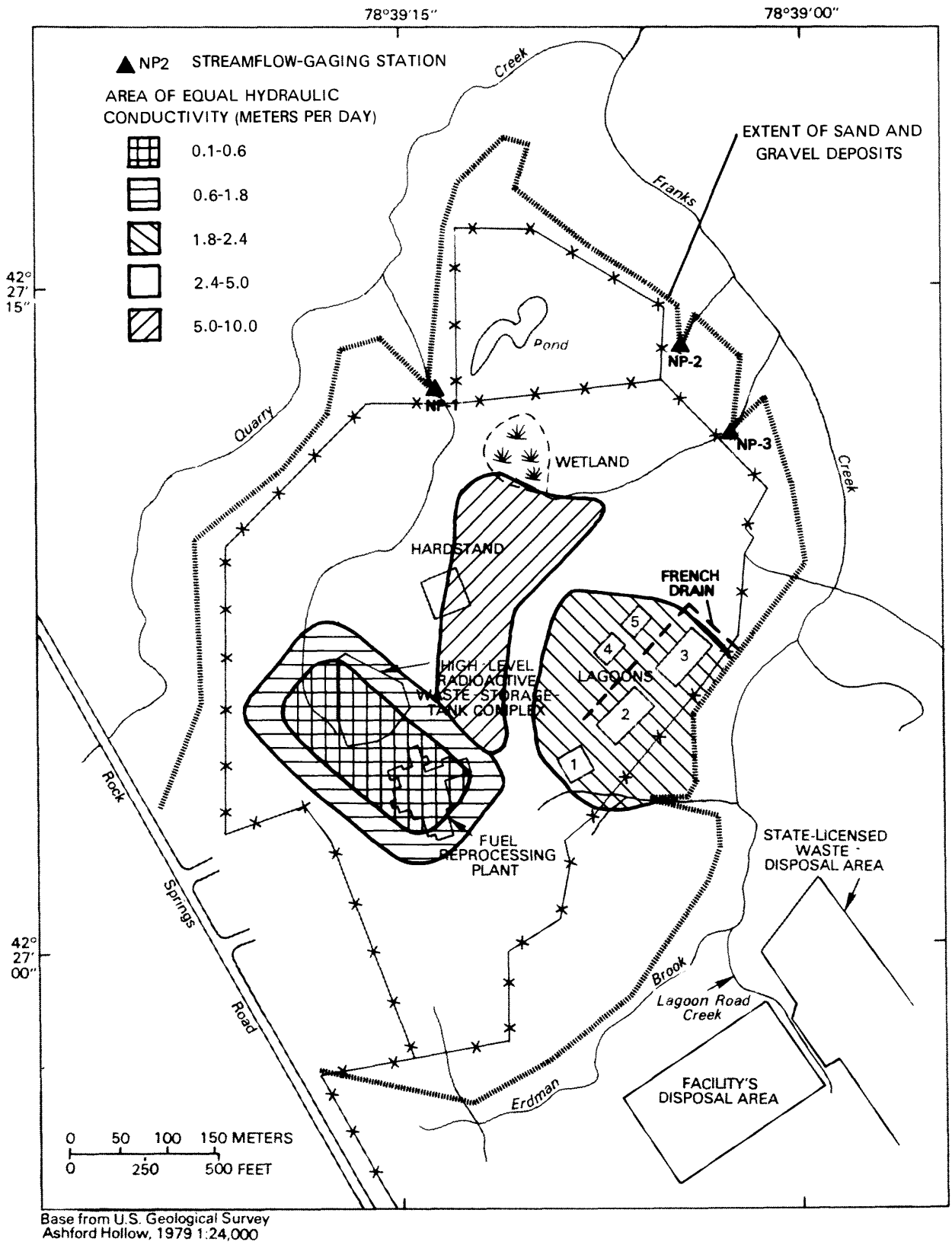

Figure 11.--Hydraulic-conductivity values used in model simulations of sand and gravel on north plateau.

Recharge

Ground water enters the sand and gravel on the north plateau as precipitation that percolates into the soil and as underflow from the fractured bedrock along the upland (southern) boundary. The estimated magnitude of flow from these sources is given in the ground-water budget in table 2. Some recharge may emanate as leakage from the main plant's outfall channel (fig. 2), underground water lines, and the leach field, but little information on these sources is available.

Annual recharge from precipitation was indicated to be 50 cm/yr by a mathematical model that simulates soil-moisture content (Steenhuis and others, 1983). The model predicted direct runoff and percolation from the soil profile through a mass-balance approach to provide a daily accounting of soil-moisture content. Soil moisture in the model was increased by precipitation and snowmelt and decreased by evapotranspiration from the root zone. Daily temperature was used to determine the timing and volume of snowmelt and evapotranspiration. The volumetric flux of water through the soil profile was calculated as a function of the soil-moisture gradient and the saturated hydraulic conductivity of the soil.

Daily values of precipitation used in the soil-moisture model were averaged from data recorded at three rain gages on the north plateau (Kappel and Harding, 1987). These values were increased by 10 percent to account for the observed surface runoff. The correction factor is similar to the magnitude-of-measurement error reported by Winter (1981, p. 86) for rain gages installed above the land surface without use of wind shields. Daily temperature was averaged from records for the three weather stations mentioned earlier, and potential evapotranspiration was calculated from the modified Penman equation mentioned previously (Steenhuis and others, 1983). A vegetative cover of grass was assumed to grow from May to October, with a maximum root-zone depth of 90 cm in July. After subtracting losses through surface runoff, the model calculated that half the 100 cm of the remaining rainfall becomes recharge, and half becomes evapotranspiration.

Table 2.--Ground-water budget for sand and gravel deposit on north plateau, October 1982 through September 1983.

[Values are in centimeters per year.]

Recharge		Discharge	
Infiltration from precipitation	50	Stream channels	13
		Springs and seepage faces	21
		French drains	
Underflow from bedrock	12	Low-level waste-treatment system	2
		Vertical leakage to till	1
Leakage from main plant's outfall channel	4	Ground-water evapotranspiration	18
		Change in storage	4
Total	66		61

Mass balance error: 8 percent

Underflow to the surficial sand and gravel was estimated from Darcy's law. If the saturated thickness of the deposit is assumed to be 1.0 m, the cross-sectional flow area near the upland boundary is 380 m^2. From figure 10, the hydraulic gradient near the boundary is 4.5 m divided by 60 m or 0.075. From an average hydraulic conductivity of 5.0 m/d, the volumetric flux, Q, is:

$$Q = (5.0 \text{ m/d})(380 \text{ m}^2)(0.075) = 142 \text{ m}^3/\text{d} \quad (1)$$

Expressed on an areal basis, annual recharge from underflow is 12 cm/yr. This estimate could be in error by a factor as great as 4 as a result of uncertainty in the saturated thickness and hydraulic-conductivity values in this area. For this reason, the volume of underflow used in the ground-water-flow model was included in a sensitivity analysis, discussed further on.

Infiltration from the plant's outfall channel, which discharges steam condensate from the main plant building to Erdman Brook, was also simulated in the model. Although this discharge is variable, a flow of 500 m^3/d was assumed representative of normal conditions on the basis of streamflow measurements. Infiltration of 10 percent of this volume would give a recharge rate of about 4 cm/yr. Potential recharge from other buried plant facilities mentioned earlier was not considered in this model.

Discharge

Ground water discharges from the surficial sand and gravel through (1) drainage to stream channels, springs, and seepage faces; (2) leakage to the french drain and the low-level waste-treatment system; (3) vertical leakage into the underlying till; and (4) evapotranspriation from the water table. The estimated magnitudes of these discharges are given in table 2.

Ground-water discharge to stream channels was estimated to be 148 m^3/d or 13 cm/yr over the entire surface area of the plateau. Discharges to stream channels were estimated from continuous streamflow values recorded at stations NP-1 and NP-3 (Kappel and Harding, 1987). Average monthly base flow at each station was determined by applying base-flow-recession techniques described in Todd (1980, p. 227) to streamflow hydrographs for October 1982 through September 1983 (Kappel and Harding, 1987).

Ground-water discharges through springs and seepage faces are difficult to measure because they occur over large, poorly defined areas. Some are intermittent and cease during the summer. The estimated discharge to springs and seepage faces of 240 m^3/d or 21 cm/yr is probably less than the actual volume because not all discharge could be measured.

Volumetric measurements of discharge from springs and seepage faces along the northeast and northwest sides of the plateau, which drain to Quarry and Franks Creeks, indicated a total discharge of 20 m^3/d or 1.8 cm/yr (Kappel and Harding, 1987). Discharges along the south side of the plateau were estimated indirectly from streamflow measurements made on Franks Creek in April 1978. These measurements indicated that flow from Erdman Brook on this side of the plateau contributed about 810 m^3/d to Franks Creek. Subtracting from this value the measured surface flow from low-level waste-burial-ground drainage

and estimated flows from the french drain and the plant-outfall channel provided an estimate of seepage from the north plateau to this tributary of 180 to 260 m^3/d (16 to 23 cm/yr).

Volumetric measurements of ground-water discharge from the french drain were made in the spring, summer, and fall of 1983. Ground-water discharge ranged from 19 to 27 m^3/d (1.7 to 2.4 cm/yr). Ground-water discharge to the low-level waste-treatment system was estimated by subtracting additions to the lagoon from the reprocessing plant and losses through evaporation from the measured increase in storage. The increase in storage in lagoon 2 was calculated for four periods from June through August 1983 during which no precipitation occurred. Ground-water discharges ranged from 9 to 40 m^3/d and averaged 26 m^3/d (2.3 cm/yr).

Vertical leakage from the surficial sand and gravel to the underlying till was estimated to be less than 1 cm/yr. The calculation was made by applying Darcy's law to a 1.0-m^2 area on the till surface. The vertical hydraulic gradient between the surficial deposit and the saturated lacustrine deposit below it is approximately 1.0 m/m. (See fig. 8B.) The saturated hydraulic conductivity of the intervening till deposit was given by Prudic (1981) as 2.0×10^{-8} cm/s (0.6 cm/yr). Vertical leakage (Q) from the sand and gravel is thus:

$$Q = (0.6 \text{ cm/yr})(1.0 \text{ m}^2)(1.0) = 0.6 \text{ cm/yr} \qquad (2)$$

Ground-water discharge through evapotranspiration includes the amount of the soil-moisture deficit that is replenished by ground water and direct evaporation where the water table is at land surface. The soil-moisture model predicted that the root zone would provide 50 cm/yr of the total evapotranspiration loss of 68 cm/yr from native grasses, mentioned earlier. Evapotranspiration losses from ground water would therefore total 18 cm/yr. This estimate would be low for areas in which the water table is at land surface and high for areas where the depth to water exceeds 1.0 m, the approximate base of the root zone.

The annual change in ground-water storage in the surficial sand and gravel was estimated from differences between water levels recorded in observation wells 80-1 through 80-8 (pl. 1) in October 1982 and those recorded in September 1983. Two wells on the upper (south) part of the plateau (80-1 and 80-2) showed an increase in water level; 80-8 showed no change, and the rest showed declines. The cumulative change indicated a net decline of 0.2 m. Assuming a specific yield of 0.20, the change in storage represents a net ground-water discharge of 4 cm/yr.

Seasonal Fluctuation of Ground-Water Levels and Discharge

Ground-water levels in observation wells fluctuate as much as 2 m during the year, and ground-water discharges to some stream channels, springs, and seepage faces can change by nearly 100 percent. Seasonal fluctuations of ground-water levels in well 80-8 south of the reprocessing plant and 80-4 near the wetland from October 1982 through September 1983 are illustrated in figure 12; base-flow discharges at two tributaries, the french drain, and springs and seeps are given in table 3.

Table 3.--Measured ground-water discharges from north plateau in March, July, and October 1983.

[Drainage area 41.4 hectares.]

Location	Measured discharge (liters per second) 3/3/83	7/5/83	10/6/83
NP-1	0.37	0.03	0.62
NP-2	.09	.03	.10
NP-3	1.76	.59	1.56
French drain at lagoons	.28	.22	.31
Springs and seepage faces	.58	.27	.62
TOTAL	3.08	1.14	3.21

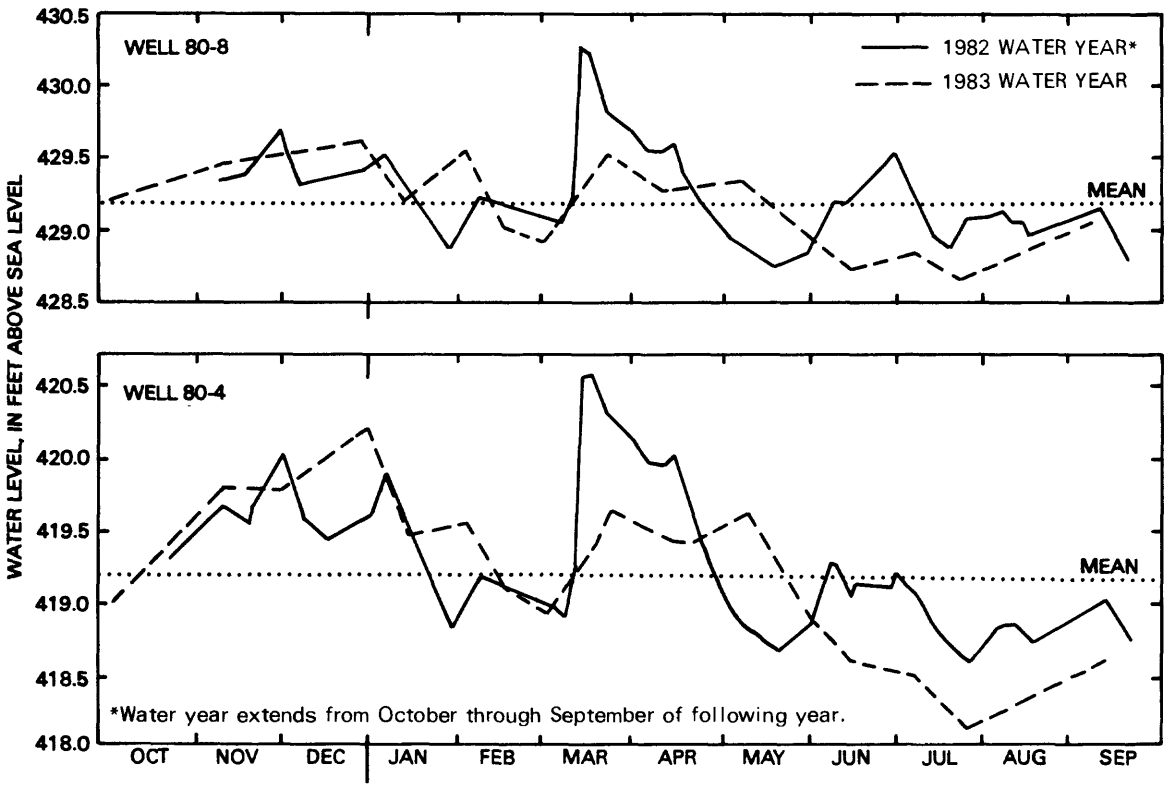

Figure 12.--Hydrographs of wells 80-4 and 80-8 on the north plateau, water years 1982-83. (Well locations are shown on pl. 1.)

Seasonal Patterns

Water levels were highest in the spring after periods of snowmelt and precipitation, when large ground-water discharges also occurred. Water levels declined during the late spring and reached the lowest level in July, when the rate of evapotranspiration was highest. Ground-water discharges generally

declined by 60 percent from March through July, although flow from the french drain remained fairly constant because the saturated thickness in that part of the north plateau was sufficient to maintain discharge throughout the year. Water levels rose with increased recharge in the fall, and ground-water discharges returned to high levels in the spring. Water levels continued to rise through the early winter until freezing temperatures began to limit recharge.

Ground-water levels and discharge fluctuate in response to seasonal variation in recharge. Precipitation falls mainly as snow from December through February and remains on land surface until it melts. Some of the snowmelt infiltrates to ground water and, when the snowpack melts in March and April, provides the greatest volume of recharge. Although brief warm spells can occur during any of the winter months, the potential for infiltration during mid-winter thaws is limited by the extent to which the soil remains frozen.

As temperatures increase and vegetation growth resumes during spring and summer, evapotranspiration removes much of the moisture held in the unsaturated zone. Evapotranspiration directly from ground water occurs in areas where the water table is near land surface. Only a small amount of precipitation recharges ground water during this period because evapotranspiration keeps the moisture content of the unsaturated zone below saturation. Recharge is possible during periods of extended precipitation, however, when the infiltration rate exceeds the evapotranspiration rate. Evapotranspiration diminishes with killing frost in the fall and thereafter allows a greater proportion of the precipitation to recharge the ground water.

Calculations of Monthly Recharge for Transient-State Model

Seasonal changes in recharge were incorporated into transient-state simulations discussed further on. Two sets of monthly recharge rates for October 1982 through September 1983 were used in the simulations; these were calculated from (1) the soil-moisture model previously mentioned, and (2) a method based on the monthly soil-moisture deficit. The latter method uses precipitation and evapotranspiration losses for each month and the annual recharge rate determined by the soil-moisture model. Evapotranspiration rates were calculated by applying a consumptive-use coefficient of 0.75 to the monthly potential evapotranspiration values, shown in figure 7. Monthly recharge rates, $RECH_i$, were then calculated by:

$$\Delta_i = \frac{PRECIP_i}{PRECIP_{avg}} (RECH_{avg} - ET_i) \qquad (3)$$

and

$$RECH_i = \Delta_i - \Delta_{min} \qquad (4)$$

where: $PRECIP_i$ = measured precipitation in month i,
$PRECIP_{avg}$ = mean monthly precipitation,
$RECH_{avg}$ = mean monthly recharge rate given by soil-moisture model,
ET_i = estimated evapotranspiration rate in month i,
Δ_{min} = minimum value of Δ for i = 1 through 12, and
$RECH_i$ = recharge applied to model for month i.

The Δ value defined by equation 3 is related to the soil-moisture deficit and weights the recharge in each month by the measured precipitation and the

estimated evapotranspiration rate. Equation 4 ensured that some recharge occurred in every month for which $\Delta_i > \Delta_{min}$ because Δ_{min} was less than zero. Recharge was assumed to be zero in July (for which $\Delta_i = \Delta_{min}$) and in January and February, when the soil was largely frozen. Potential recharge from the latter 2 months was assumed to occur in March.

Monthly recharge calculated by the soil-moisture model was greatest in March and declined to zero by June. A lesser amount of recharge was calculated for September through December. Recharge calculated by the soil-moisture-deficit method was distributed more uniformly through the year. Monthly recharge rates calculated by the two methods are presented in figure 13.

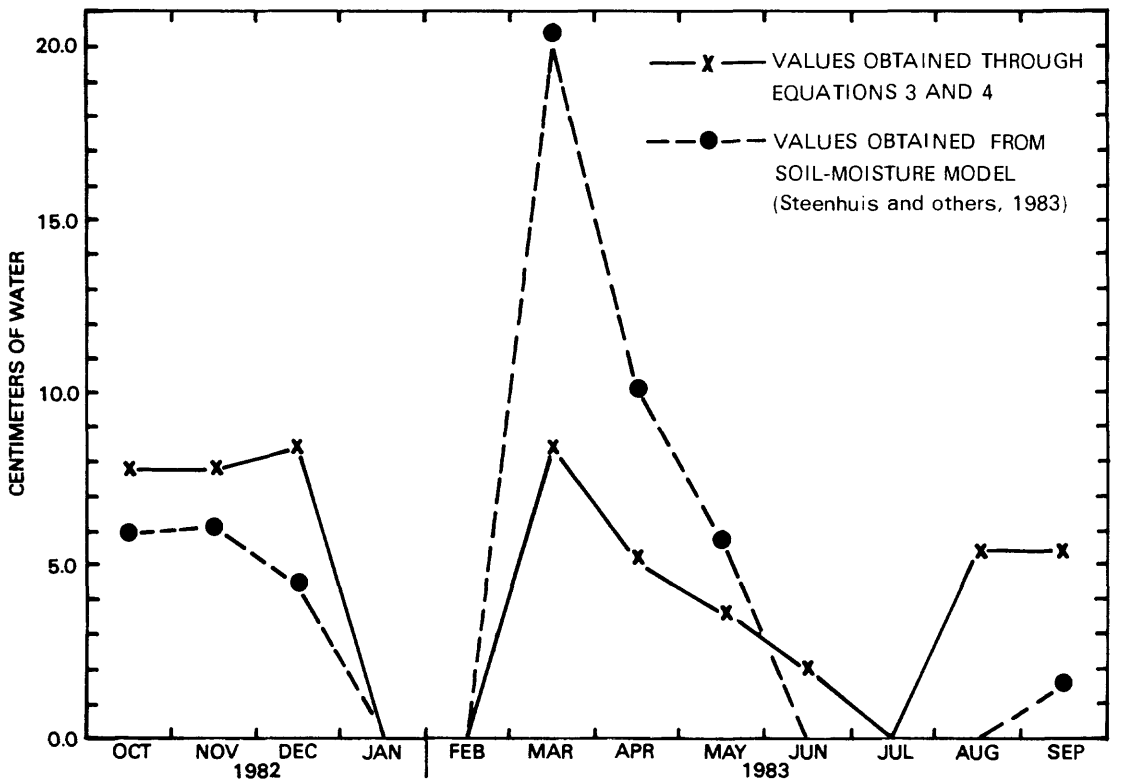

Figure 13.--Monthly recharge rates, 1982-83, calculated by equations 3 and 4 and by soil-moisture model used in transient-state simulations.

SIMULATION OF GROUND-WATER FLOW

The ground-water flow model developed in this study was calibrated to ground-water levels and discharges measured on the north plateau during 1982-83. By calculating ground-water flow paths and velocities through the surficial sand and gravel deposit, the model can be used to predict travel-times of conservative solutes in the ground water. The model was calibrated through steady-state simulations that represented average flow conditions and transient-state simulations that incorporated the effects of storage during a 1-year period, October 1982 through September 1983).

Flow Model

Ground water in the surficial sand and gravel on the north plateau is unconfined and flows laterally, parallel to the surface of the underlying till. Ground-water flow in this system can be described by the following partial differential equation governing two-dimensional flow through a porous medium:

$$\frac{\partial}{\partial x} T_{xx} \frac{\partial h}{\partial x} + \frac{\partial}{\partial y} T_{yy} \frac{\partial h}{\partial y} - W = S_y \frac{\partial h}{\partial t} \qquad (5)$$

where: x and y = cartesian coordinates aligned on the major axes of transmissivity, T_{xx}, T_{yy},
h = hydraulic head (L),
W = volumetric flux per unit area representing sources and/or sinks of water (L/t),
S_y = specific yield (dimensionless), and
t = time (t).

The model used in this study solves a set of finite-difference approximations to this equation. It uses a grid to divide the aquifer system into an array of rows and columns. A complete discussion of the model derivation is given in McDonald and Harbaugh (1984).

Design

The north plateau area was simulated on a finite-difference grid that represents an area of 41.4 ha. The model grid (fig. 14) contains 644 cells (23 rows by 24 columns), of which 202 are inactive. Each grid cell represents 30.5 x 30.5 m, roughly 1/10 ha.

Model boundary conditions were selected to approximate the effect of real hydrologic bondaries. The types and locations of boundaries used in the model are indicated in figure 14. No-flow boundaries were specified to correspond to the high-level liquid-waste-tank complex and the main plant building. The surface of the underlying till was also treated as a no-flow boundary because the quantity of flow through this unit represents less than 2 percent of the estimated ground-water discharge from the north plateau (table 2).

The surficial sand and gravel is recharged by underflow from bedrock west of the main plant building along Rock Springs Road (fig. 14). This boundary was initially represented in the model by constant-head cells in which the water table was maintained at a constant level, and later represented by constant-flux cells. The volume of underflow entering the surficial gravel at each constant-flux cell was determined by the model with the constant-head boundary. A range of constant fluxes was then used with the steady-state model to test the effect of underflow on the predicted hydraulic-head distribution. Constant-flux cells were also used to simulate leakage from the outfall channel that drains the main-plant area.

Ground water discharges from the plateau to stream channels upstream from stations NP1, NP2, and NP3, the french drain, and the low-level waste-treatment system (fig. 3) and also through seepage faces along the edges of the plateau. These discharge points were simulated in the model by drains. Each drain assigns seepage from a grid cell at a rate proportional to the difference in

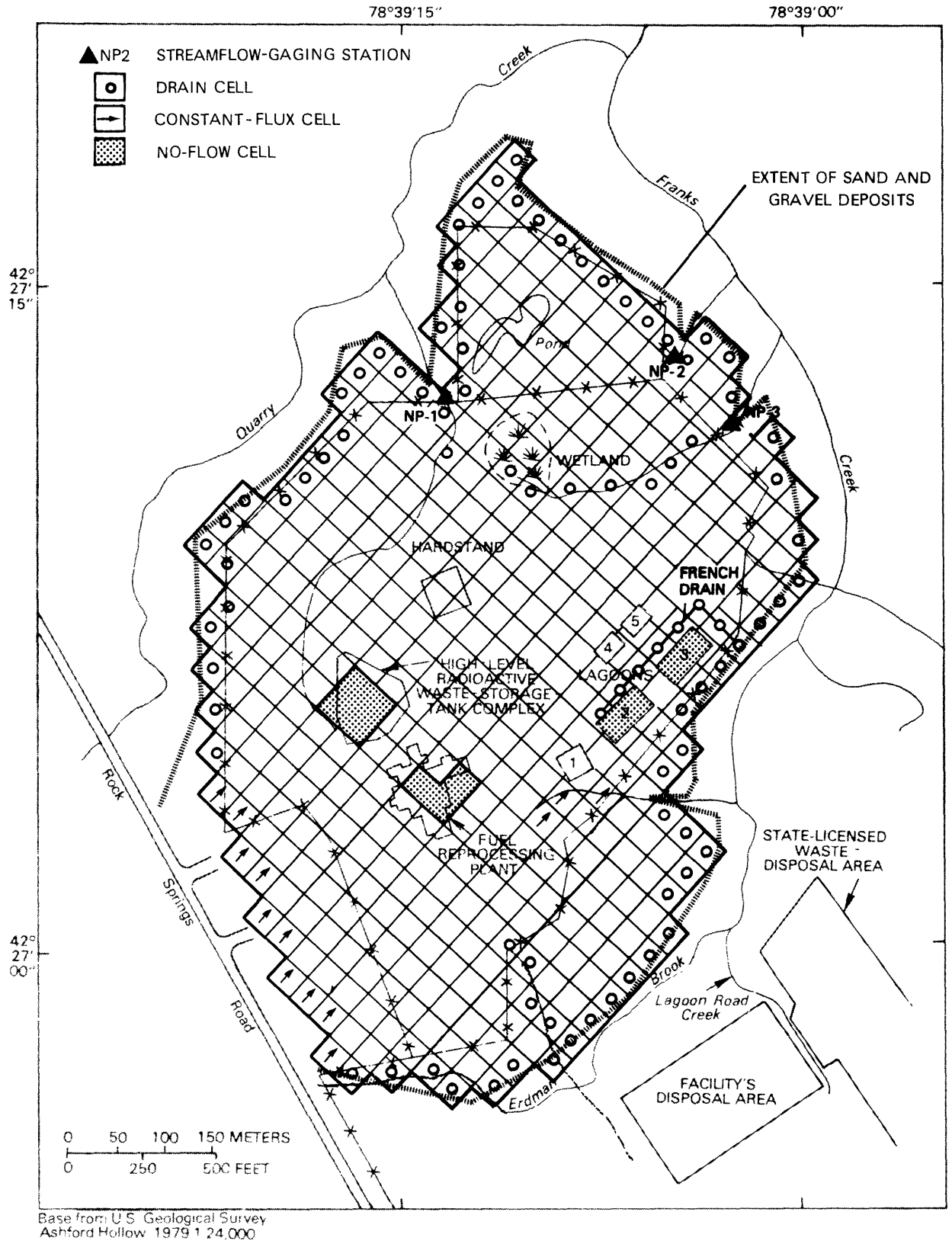

Figure 14.--Finite-difference grid and boundary conditions used in model simulations.

altitude between the water table and the drain. The model calculates the rate of seepage through the equation:

$$Q = C(h-d) \quad (6)$$

where: Q = seepage rate (m^3/d),
C = conductance of the interface between the aquifer and the drain (m^2/d),
h = hydraulic head in the aquifer (m), and
d = elevation of the drain (m).

Drain conductance was defined as:

$$C = \frac{AK}{l} \quad (7)$$

where: A = average cross-sectional flow area (m^2),
K = hydraulic conductivity of the interface (m/d), and
l = flow path length (m).

Drain altitudes used in the model were assumed to be 0.3 m above the surface of the till to provide sufficient saturated thickness for seepage to occur. Estimation of drain conductance is described in the discussion of hydraulic conductivity further on.

Input Data

Hydraulic Conductivity.--Hydraulic conductivity of grid cells ranged from 0.6 to 10.0 m/d, in accordance with the distribution shown in figure 4. The model computed saturated thickness of each grid cell by subtracting the altitude of the bottom of the gravel deposit from the altitude of the simulated water-table surface. The bottom altitude of the surficial gravel was determined from a contour map of the surface of the upper till unit (Albanese and others, 1983). Altitudes of the till surface at the edge of the plateau were interpolated from the altitudes of springs shown in figure 10.

Hydraulic conductivity of the surficial sand and gravel was used to estimate the conductance term, C, in equation 6. McDonald and Harbaugh (1984) discuss a variety of factors that may affect drain conductance, including the thickness of the interface between the aquifer and the drain, and the difference in permeability between the aquifer material and drain material. No information on the hydraulic properties of the interface was available. Drain conductance was estimated on the assumption that the length of the flow path through the interface was 0.3 m. The hydraulic conductivity of the interface was assumed to be 0.03 m/d, which is within the range of values for fine sand and silt (Todd, 1980, p. 71). Diagrams of the cross-sectional areas used to estimate conductance of the four types of drains simulated by the model are shown in figure 15. Initial estimates of drain conductance were modified during calibration to improve model predictions of ground-water discharge and hydraulic head.

Recharge and Evapotranspiration.--Ground-water recharge was assumed to occur at a uniform rate across the north plateau. The amount of recharge applied to each grid cell totaled 50 cm/yr, the value obtained from the soil-moisture model mentioned earlier. This rate was later adjusted during calibration to determine model sensitivity to recharge.

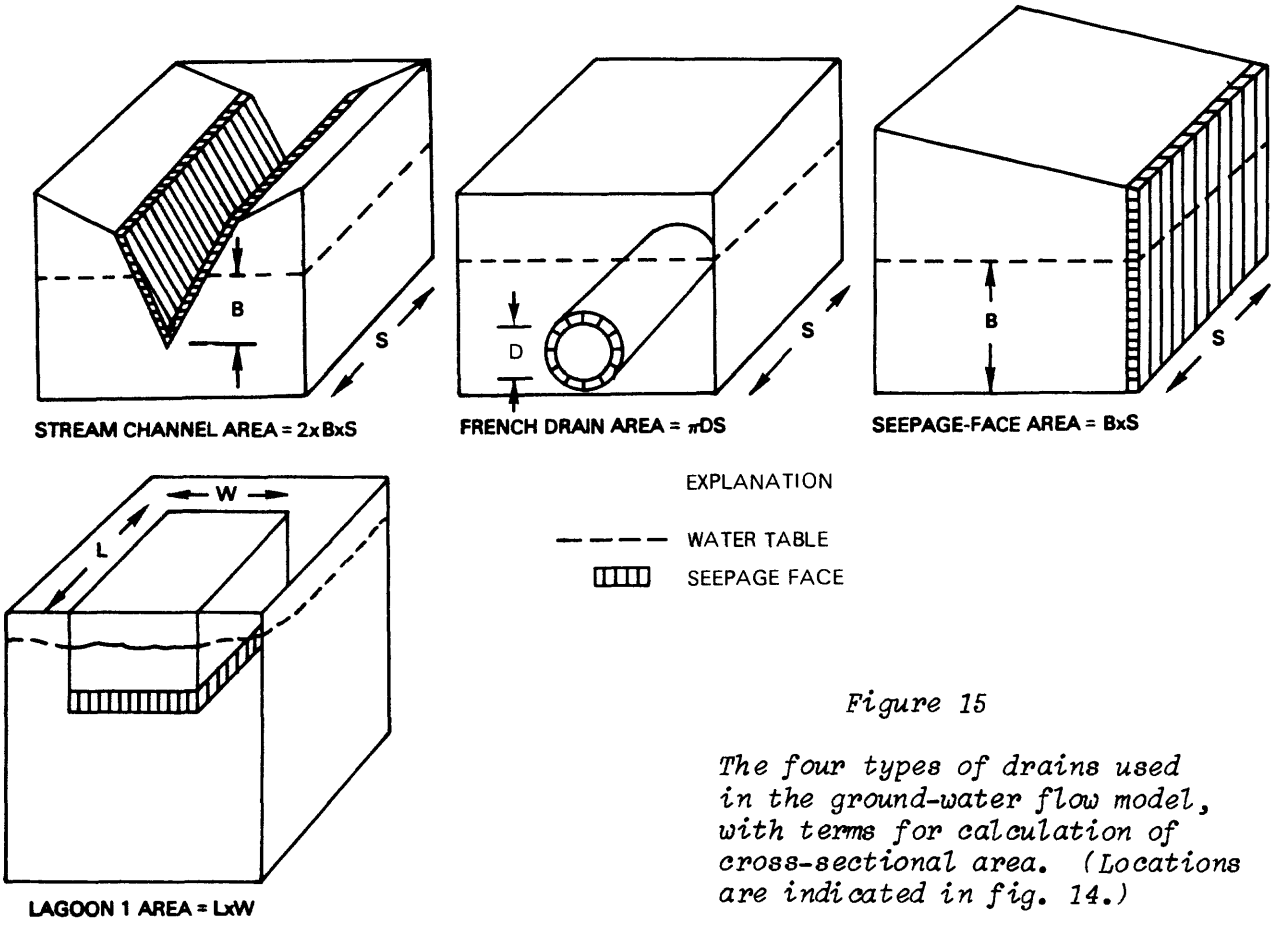

Figure 15

The four types of drains used in the ground-water flow model, with terms for calculation of cross-sectional area. (Locations are indicated in fig. 14.)

Evapotranspiration from ground water on the north plateau is not uniform but depends upon the depth of the water table. Evapotranspiration from each grid cell in the model was determined from the function illustrated in figure 16. No evapotranspiration occurred in grid cells where the water table was below the root zone, which was estimated to be 1 m thick. In grid cells where the water table was at or above the land surface, evapotranspiration was assumed to occur at the actual evapotranspiration rate. For water levels within the root zone, the evapotranspiration rate was proportional to the depth to water.

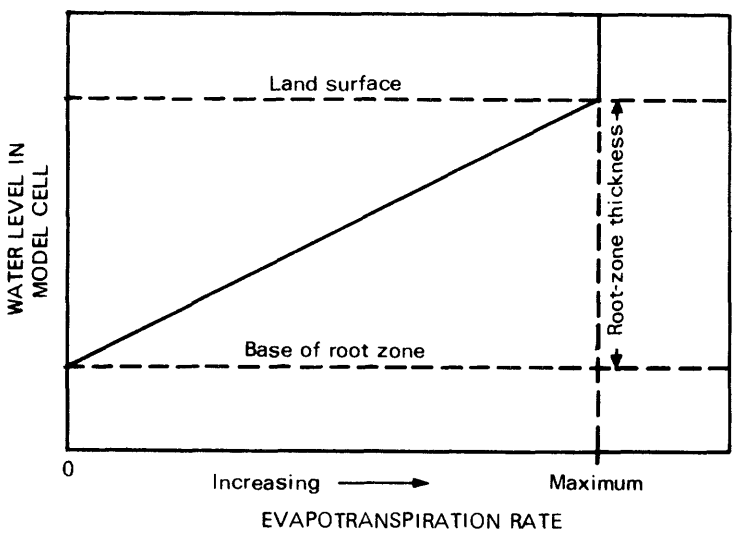

Figure 16

Relationship between water level in model cell and evapotranspiration rate. (Modified from McDonald and Harbaugh, 1984, p. 317.)

The plant facilities and associated paved areas prevent recharge and evapotranspiration over a significant area of the plateau. Active grid cells in which recharge and evapotranspiration were not allowed to occur are indicated in figure 17.

Steady-State Simulations

Steady-state simulations were uased to calibrate the ground-water-flow model to predict the mean annual water-table altitude. For the purpose of this study, the simulated head distribution was compared with ground-water levels measured in 23 observation wells on May 10, 1983, when water levels were close to the mean of levels recorded from October 1981 through September 1983 (fig. 12). During this period, the total precipitation (92 cm) was slightly lower than the mean annual rate of 100 cm/yr. Simulated ground-water discharges were compared with mean daily discharges derived from the annual discharges of stream channels above stations NP1, NP2, and NP3, and the french drain.

Calibration

The model was calibrated by comparing simulated ground-water levels and ground-water discharges with those observed in the field. The calibration procedure entailed trial-and-error adjustments of boundary conditions and hydraulic conductivity, drain conductance, recharge, and potential evapotranspiration. Values were selected to cover the range of uncertainty associated with each term. Progress in model calibration was measured by the mean absolute difference of estimate between the simulated and observed hydraulic head in the 23 observation wells, and the root-mean-square difference of estimate between simulated and observed discharges into the NP1 and NP3 channels and the french drain.[1]

Sensitivity

Optimum coefficients obtained with the steady-state model are presented in table 4, which also summarizes the results of sensitivity testing to evaluate each term's relative effect on simulated ground-water levels and discharges. Results of 10 steady-state simulations are listed, in which the calibrated value of a single variable was changed while the values of the

---

[1] Mean absolute difference $= \sum_{i}^{n} \frac{(O_i - P_i)}{n}$,

root-mean-square difference $= \left[\sum_{i}^{n} \frac{(O_i - P_i)^2}{O_i} \right]^{1/2}$

where: O_i = observed value at point i,
P_i = predicted value at point i,
n = number of points.

Table 4.--Optimum values obtained through steady-state simulation and results of sensitivity analysis.

Variable	Steady-state optimum range	Values tested in sensitivity analysis: Recharge	Hydraulic conductivity	Drain conductivity	Underflow
Recharge (m/yr)	0.46	0.42, 0.74	--	--	--
Maximum evapotranspiration rate (m/yr)	.60	--	--	--	--
Hydraulic conductivity (m/d)	.6-10.0	--	[a]5.0, 0.3-5.0, 1.2-20.0	--	--
Drain conductivity[b] (m/d)	.003	--	--	[c]0.015, [c]0.06, [d]0.06	--
Underflow (m/yr)	.11	--	--	--	0.055, 0.22
Simulated evaporation losses from ground water (m/yr)	.20	0.14,0.28	0.30, 0.29, 0.36	0.29, 0.18, 0.11	0.25, 0.37
Difference between observed and simulated values					
Ground-water levels (m)	.51	.75, .64	.77, .85, .60	.54, .60, .66	.73, .77
Ground-water discharges (percent)	4	18, 18	18, 23, 21	32, 15, 16	12, 9

[a] Uniform value for all grid cells
[b] Drain conductances were incorporated in cross-sectional flow areas shown in figure 11.
[c] Channels above NP-1 and NP-3 only
[d] Seepage faces only

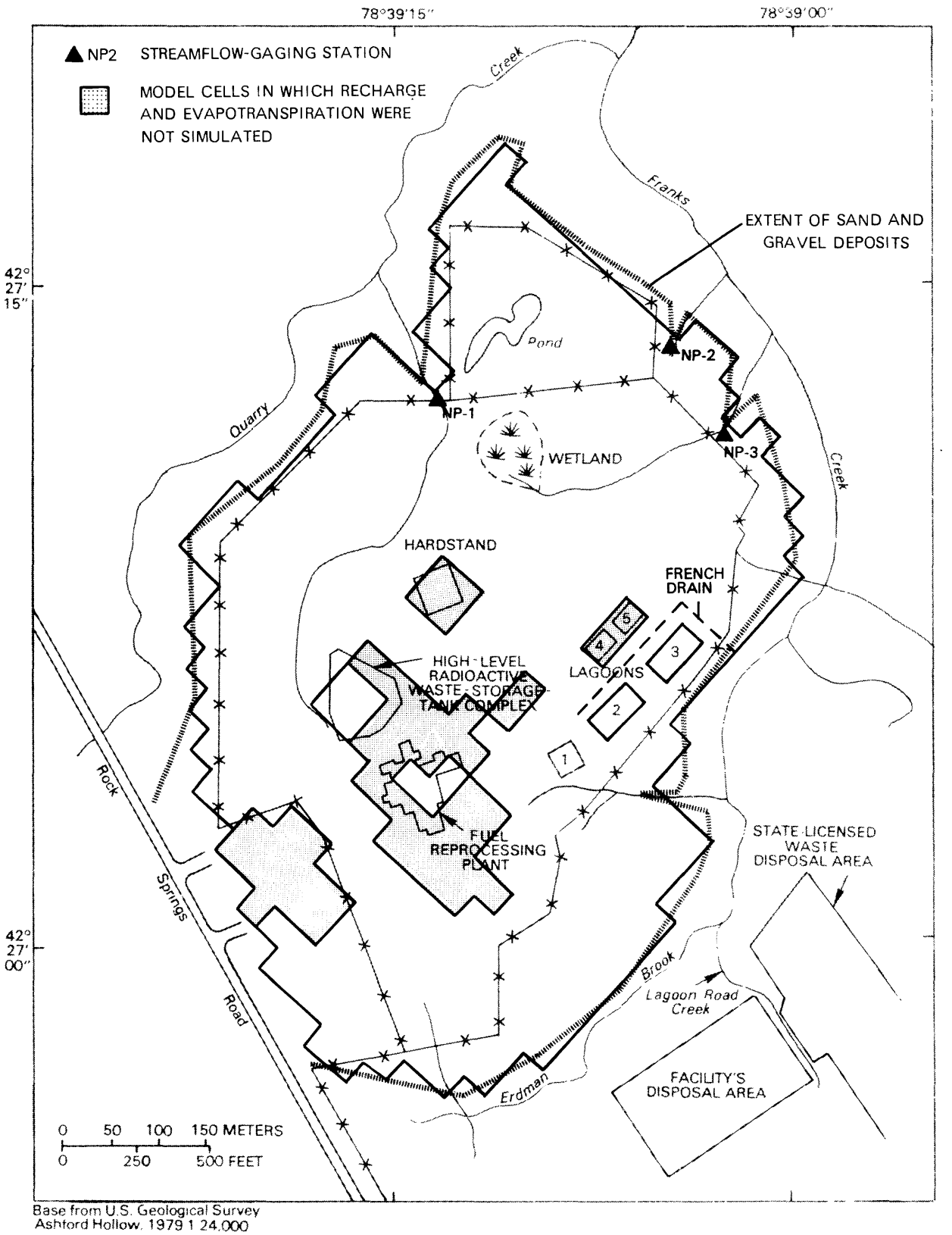

Figure 17.--Model cells in which recharge and evapotranspiration were not simulated.

other four variables were held constant. The table includes the simulated ground-water evapotranspiration value calculated for each simulation and the resulting difference between observed and simulated values of water levels and discharges.

Ground-water evapotranspiration served to reduce the effect of changing the optimum values. In simulations that produced higher water levels than were obtained with the optimum values, ground-water evapotranspiration increased, which limited the resulting rise in water levels. Similarly, in simulations in which water levels were lower, ground-water evapotranspiration decreased. The effect was that water levels were restricted to a fairly narrow range in all simulations used in the sensitivity analysis.

Recharge was the term to which the model was most sensitive in steady-state simulations. Table 4 indicates that reducing ground-water recharge by 10 percent from 46 to 42 cm/yr increased the difference between simulated and observed water levels from 0.51 to 0.75 m and the difference between simulated and observed ground-water discharges from 4 to 18 percent. Decreasing recharge also caused parts of the simulated area to go dry. Changes in recharge also affected the volume of ground-water discharges. In general, the lower values of recharge could not produce the discharges observed in the stream channels at NP-1 and NP-3 nor those in the french drain.

Average hydraulic-conductivity values of the surficial gravel used during steady-state calibration ranged from 0.6 m/d to 10.0 m/d. Decreasing the optimum values of hydraulic conductivity by 50 percent increased predicted ground-water levels by 1 m and produced much smaller ground-water discharges than those observed. Doubling the optimum values lowered ground-water levels and dewatered parts of the plateau. The spatial distribution of hydraulic conductivity used in steady-state simulations significantly improved model predictions. This can be seen by comparing errors associated with the optimum model run with that based on a uniform hydraulic-conductivity value of 5.0 m/d (table 4).

Changes in drain conductance affected the ground-water discharges and some water levels near the seepage-face boundary. Discharge into the low-level waste-treatment system was extremely sensitive to changes in water level. A water-level decline of about 0.3 m caused a nearly fivefold decrease in discharge. This predicted decrease in discharge agrees with the estimated decrease in seepage losses to the lagoon during a period when the water table declined by a similar amount.

The steady-state model was also sensitive to changes in underflow through the upland boundary. Doubling the underflow caused water levels to rise 1 to 2 m in the upper (south) part of the plateau and greatly increased the rate of evapotranspiration. Decreasing underflow by 50 percent lowered water levels by a similar amount and dewatered a large section of the plateau.

Results

Water-level altitudes computed by the steady-state model and those measured on May 10, 1983 are plotted in figure 18. The mean absolute difference between computed water levels and those measured in the field is 0.5 m,

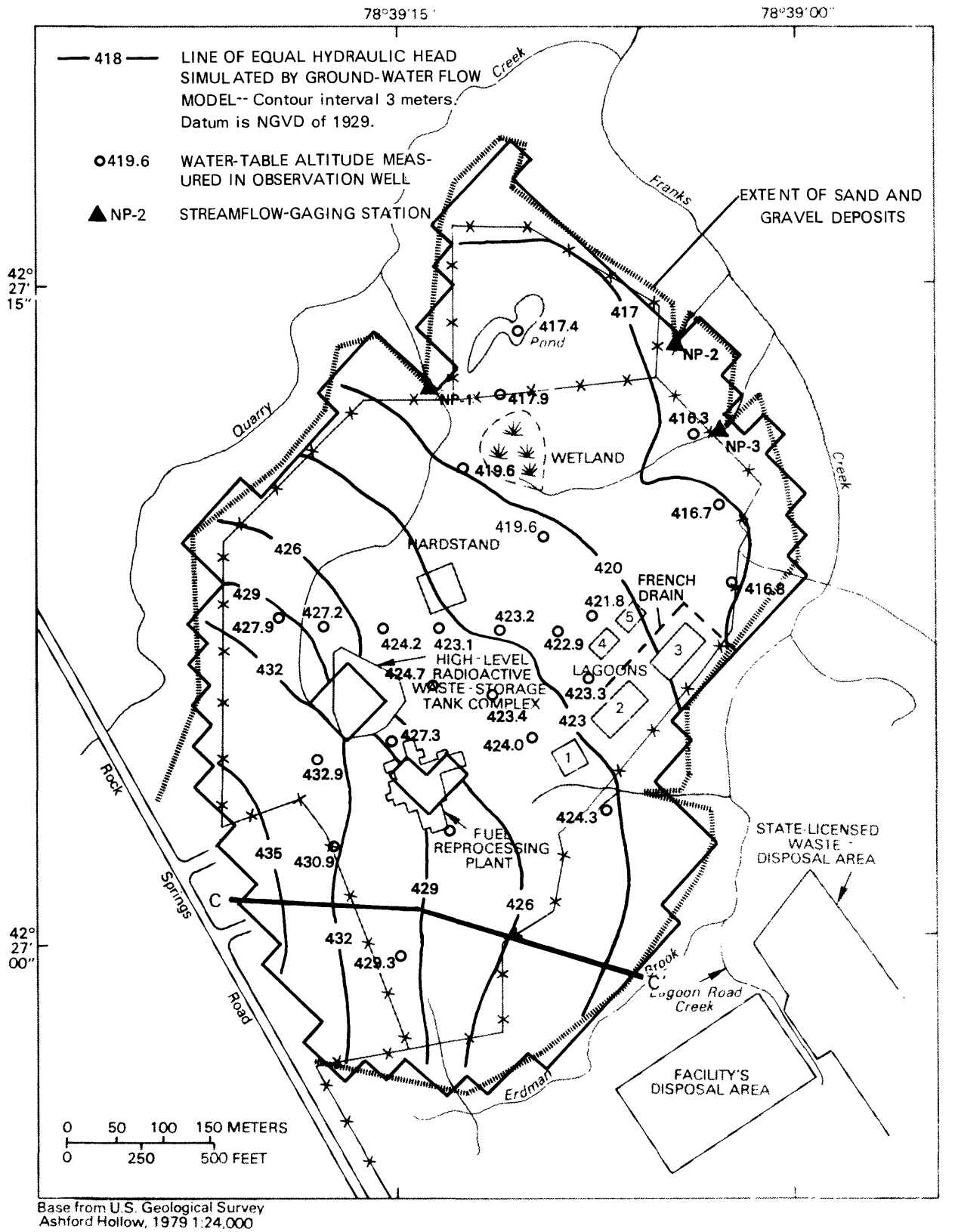

Figure 18.--Simulated steady-state and measured water levels on the north plateau.

which is less than 5 percent of the 16-m difference between hydraulic head measured at the highest and lowest points on the plateau. Ground-water levels computed by the model are within 1.5 m of water levels measured in the 23 observation wells. The principal inflows and discharges of ground water predicted by the model are listed in table 5. The root-mean-square difference between measured and simulated ground-water discharges to stream channels upstream from stations NP1 and NP3 and the french drain was 4 percent. Discharges to the low-level waste-treatment system and the Franks Creek tributary compared favorably with spot measurements made at these points.

The ground-water budget computed by the steady-state simulations closely parallels the budget given in table 3 (p. 24). The areal recharge rate of 46 cm/yr used was nearly 50 percent of the measured precipitation and slightly lower than the 50 cm/yr predicted by the soil-moisture model. Underflow from upland sources was estimated to be 17 percent of the total recharge. Combined discharge through seepage faces was nearly twice the discharge to the channel above station NP-3. Evapotranspiration from the water table was estimated to be 20 cm/yr. Including evapotranspiration from the root zone would give a total annual rate of 70 cm/yr, or 77 percent of the calculated potential rate. This agrees closely with the evapotranspiration estimate obtained from the Penman equation, as described earlier.

Table 5.--Recharge and discharge values calculated by steady-state model.

[All values are in centimeters per year]

Recharge sources		Discharge sites	
Infiltration from precipitation	46.0	Evapotranspiration	20.0
		NP-1 channel	2.2
Underflow from bedrock	10.4	NP-3 channel	10.0
Leakage from outfall channel	3.7	French drain	2.1
		Low-level waste treatment system	2.2
		Franks Creek tributary	14.5
		Other seepage faces	9.0
TOTAL	60.1		60.0

The distribution of discharge rates simulated by the model is plotted in figure 19; the distribution of evaporation is shown in figure 20. The main discharge areas were on the southeast boundary of the plateau along Erdman Brook and on the northern part of the plateau near the NP-1 and NP-3 channels. Evapotranspiration from the water table, which is restricted to areas where the depth to water is less than 1 m, occured mainly in the wetland area on the north plateau and along the north boundary near the seepage faces.

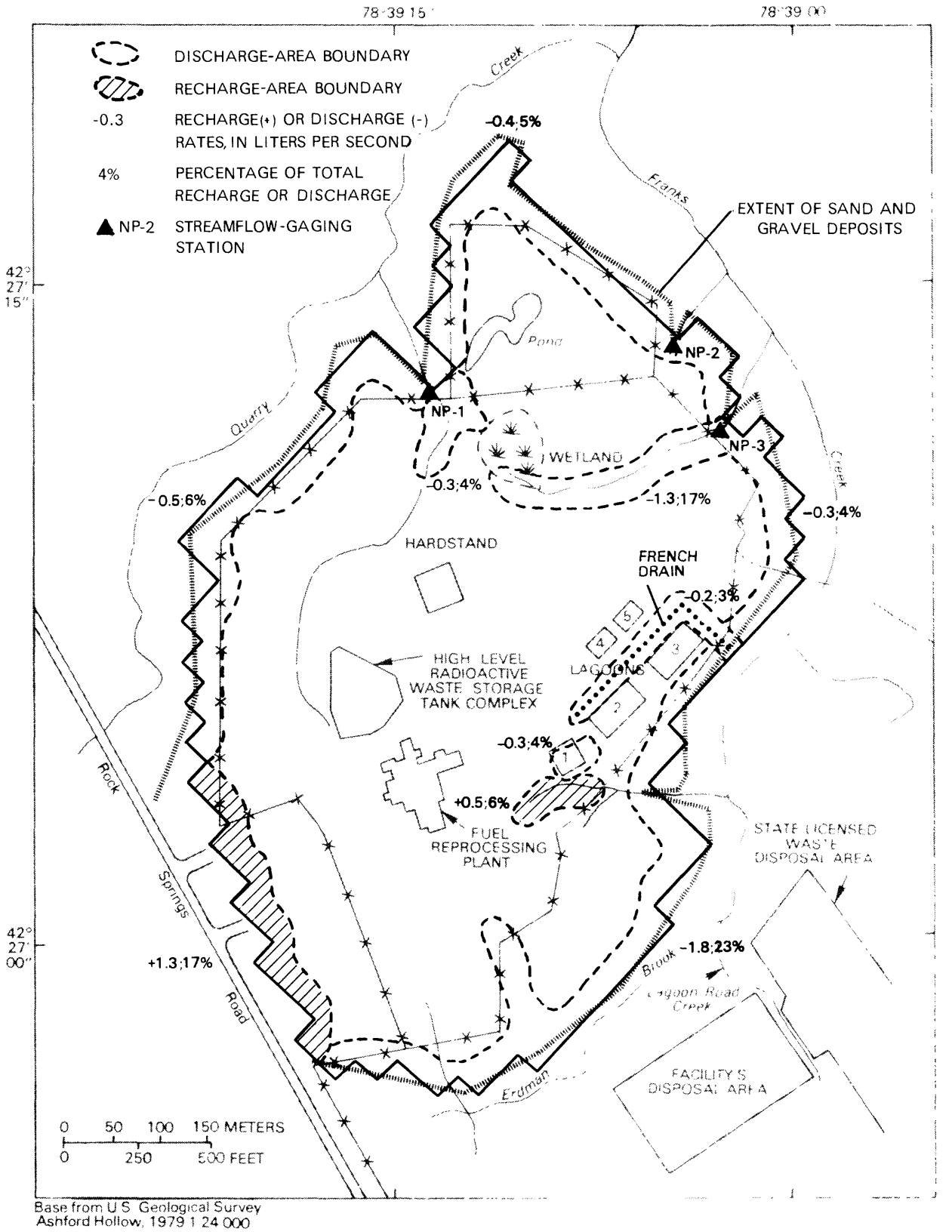

Figure 19.--Predicted steady-state rates of recharge and discharge from contant-flux and drain boundaries.

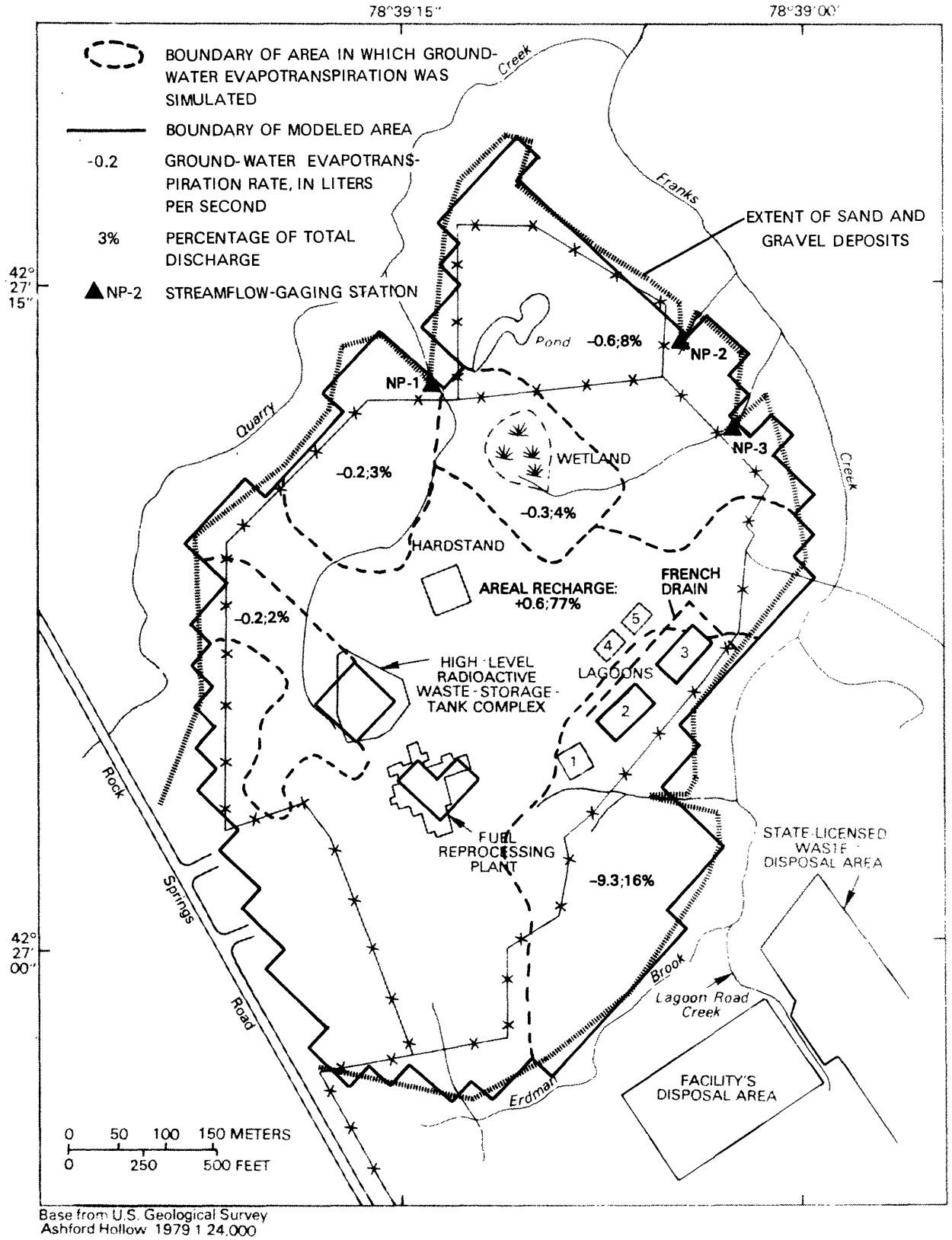

Figure 20.--Predicted steady-state distribution of evapotranspiration.

The most significant discrepancies between the hydraulic-head distribution generated by the model and the measured water-table altitude were near seepage faces along the plateau's southeastern perimeter. Water levels generated by the model were 2 to 3 m above land surface in several grid cells along this discharge boundary. This difference is attributed to the uniform grid spacing selected for the model, which resulted in an abrupt change in average saturated thickness along a flow path approaching the boundary. Decreasing the grid spacing by 50 percent along this boundary lowered the simulated water levels by 1 to 2 m, as shown in figure 21.

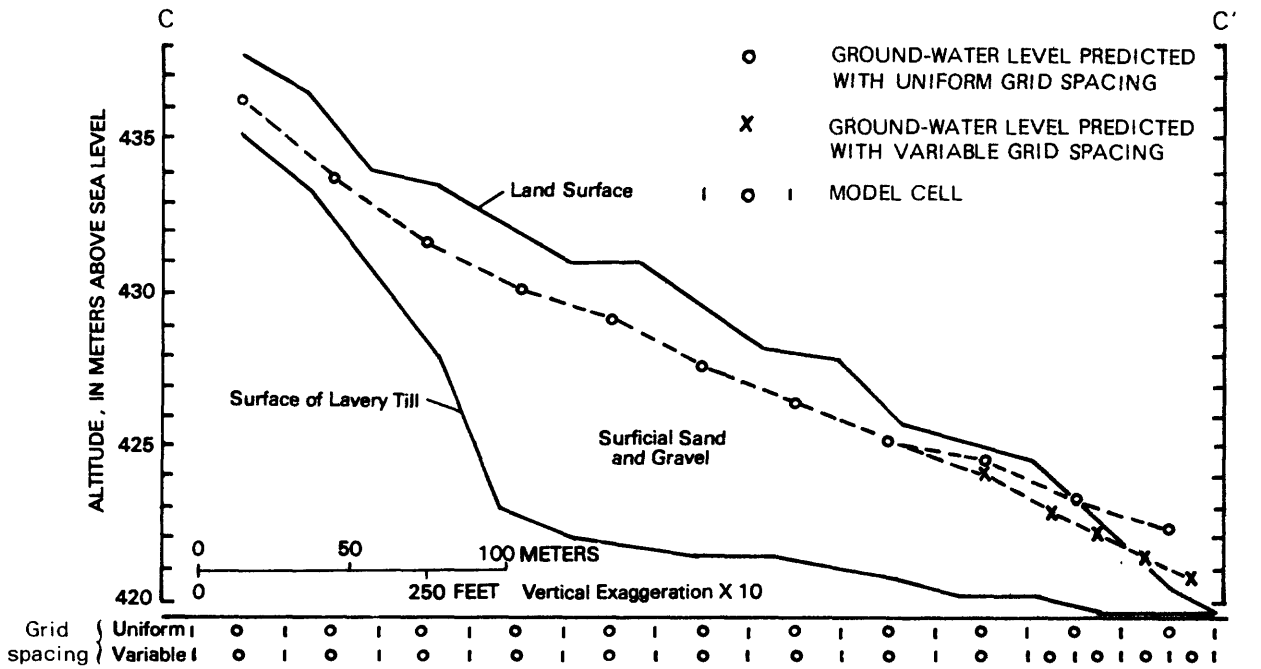

Figure 21.--Simulated ground-water levels near a seepage face based on variable-grid and uniform-grid spacing. (Location of section shown on fig. 18.)

Transient-State Simulations

Transient-state simulations of the ground-water-level response to variations in monthly recharge and evapotranspiration were used to estimate the specific yield of the surficial sand and gravel and to verify the hydrologic values obtained from steady-state simulations. Transient-state simulations represented an annual climatic cycle beginning in October 1982, a period when water levels were close to the mean levels used to calibrate steady-state simulations. The hydraulic-head distribution computed by the calibrated steady-state model was the initial condition used in the transient-state simulation. The transient simulation was divided into 12 one-month periods for which average monthly values of evapotranspiration, recharge, and underflow were specified. Each monthly period was simulated as four time steps to dampen the effect of abrupt changes in recharge from month to month. A 2-year period was simulated by repeating the annual cycle to minimize the effect of error in the initial water levels specified in the transient-state model.

Calibration

Ground-water levels computed by transient-state simulations were compared with average monthly levels recorded in wells 80-1 through 80-8 from October 1982 through September 1983, and computed ground-water discharges to streams were compared with base-flow hydrographs recorded at stations NP1 and NP3. The sensitivity of predicted water levels to changes in storage was tested through a range of specific yield values, and the sensitivity of water levels to monthly recharge was tested through the two sets of monthly recharge rates given in figure 13. Underflow through the upland boundary of the modeled area was adjusted by a factor proportional to the recharge assumed to occur in each month.

Sensitivity

Water levels computed by the transient-state model were sensitive to monthly recharge rates and less sensitive to specific yield. Comparison of computed with observed water levels at wells 80-3 through 80-6 (fig. 22) shows that the computed water levels follow the observed seasonal fluctuations but are of lesser magnitude. The discrepancy between computed and observed water levels can largely be attributed to error in the timing and amount of recharge specified in the transient-state model; water levels were also affected by the value of specific yield (fig. 23). The lower value of specific yield (0.10) produced a close approximation of the large water-level fluctuations recorded in wells 80-4, 80-5, and 80-6, whereas a specific yield of 0.20 produced a better match for the other wells.

Computed base flow at stations NP1 and NP3 was sensitive to drain conductance (fig. 24). Ground-water discharges predicted from average drain conductances obtained through steady-state simulations did not correspond closely to the estimated base flow at these two stations. The discrepancies between computed and observed discharges can largely be attributed to seasonal changes in drain conductance. As shown in equation 6 and figure 15, drain conductance is directly proportional to the average cross-sectional flow area entering the drain and therefore to the height of the seepage face on the channel bank. Because the saturated thickness of the surficial gravel draining to the stream channel varies throughout the year, the conductance of the channels can be assumed to vary as well.

In a separate transient-state simulation, drain-conductance values for each month were adjusted by a factor proportional to the saturated thickness of adjacent grid cells computed in a previous simulation that assumed constant drain conductance. The discharges at stations NP-1 and NP-3 predicted from variable drain conductances were closer to the observed base-flow values and did not substantially alter the resulting water-level hydrographs (fig. 24).

Results

Hydrographs of measured and simulated ground-water levels at wells 80-1 through 80-8 are presented in figure 25; measured and simulated ground-water discharges to channels above stations NP-1 and NP-3 are plotted in figure 24. Model predictions were obtained from the set of optimum hydrologic values listed in table 4, the set of monthly recharge rates calculated from equations 3 and 4, and values of specific yield ranging from 0.10 to 0.20.

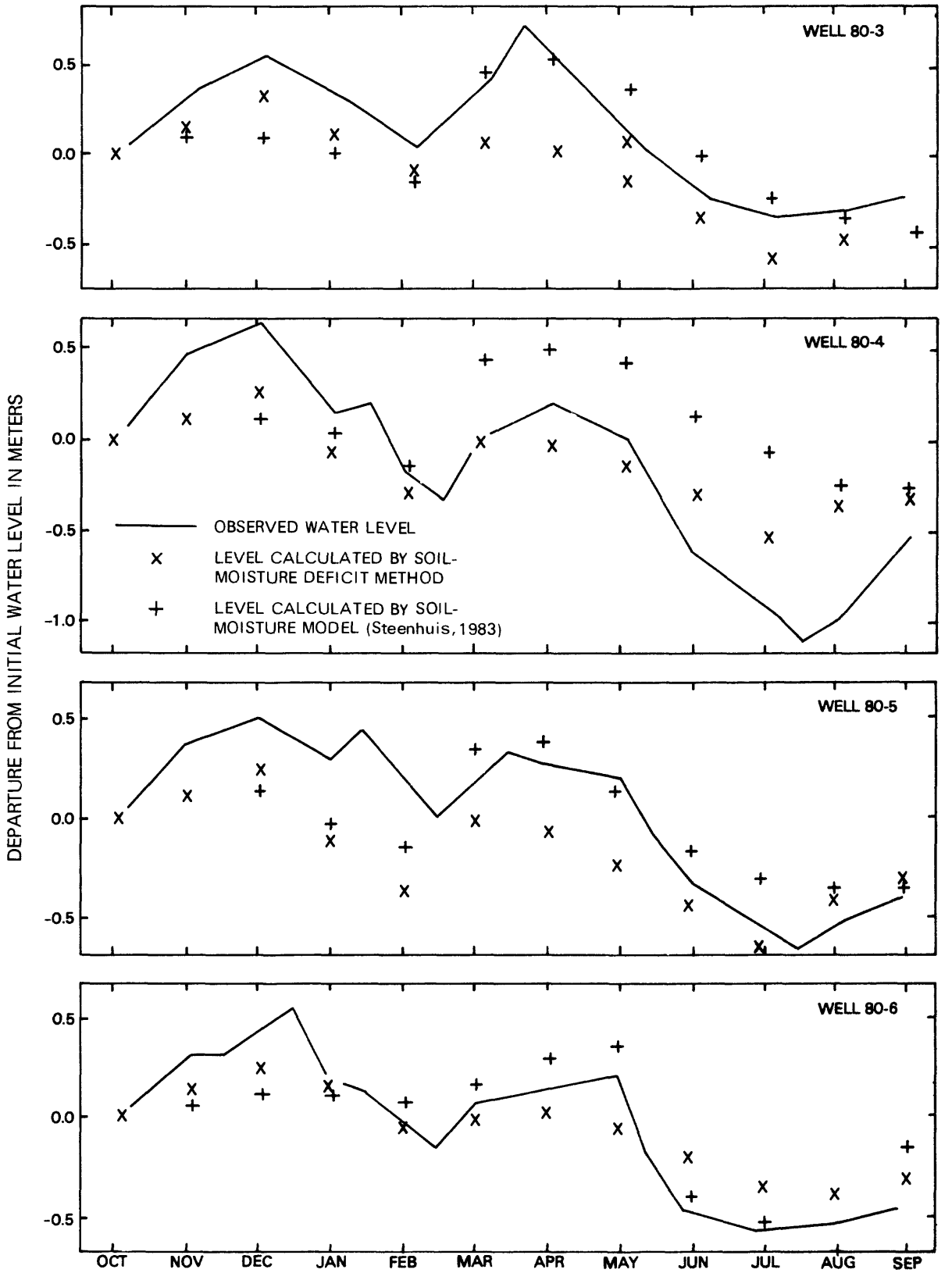

Figure 22.--Observed ground-water levels in four wells in relation to seasonal recharge computed by soil-moisture-deficit method and by soil-moisture model of Steenhuis and others (1983).

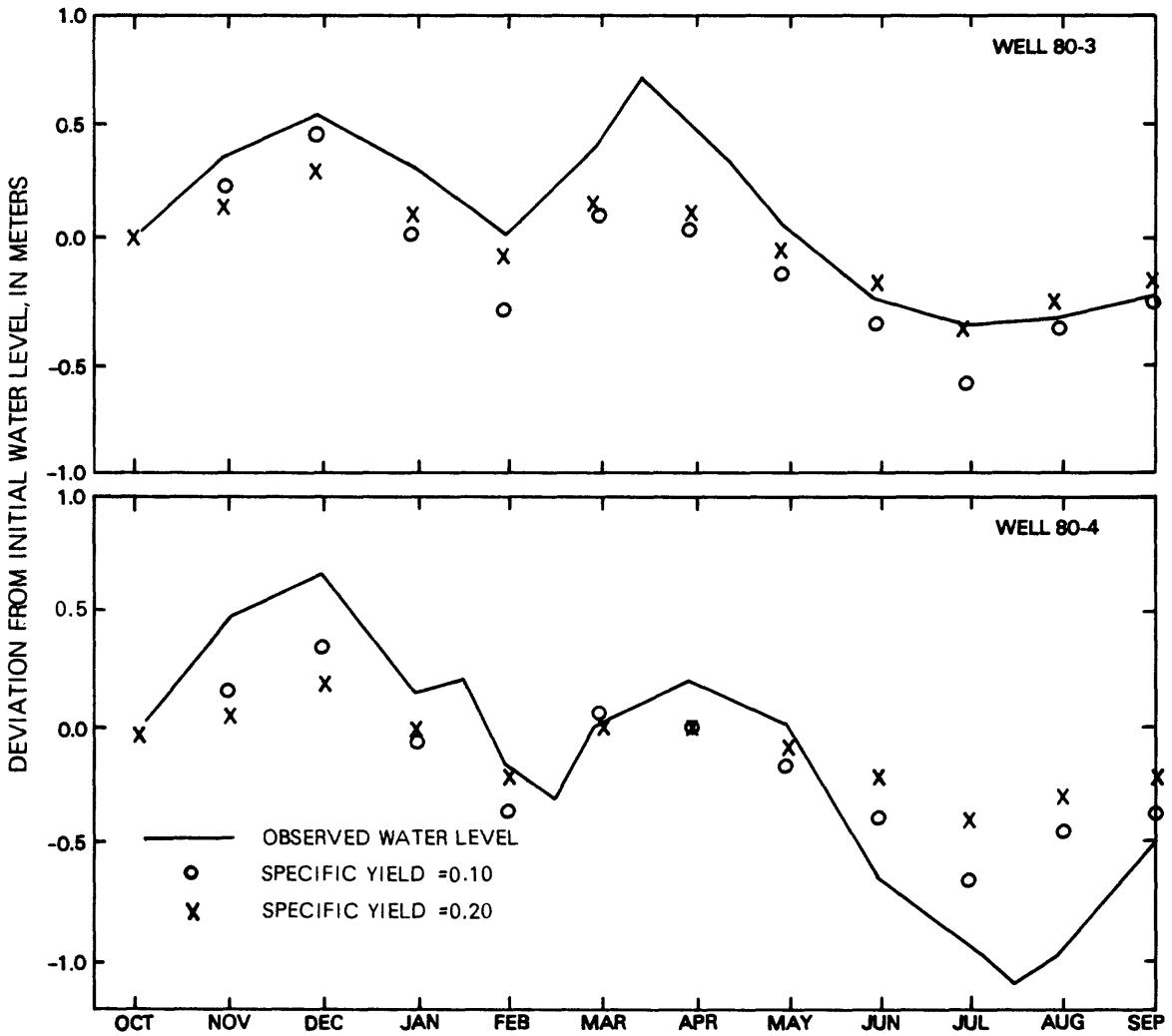

Figure 23.--Observed departures of ground-water levels from initial level at wells 80-3 and 80-4 in relation to simulated values computed from two magnitudes of specific yield.

The well hydrographs generated by the transient-state model (fig. 25) closely correspond to recorded water levels. Simulated ground-water discharges follow the annual pattern of high flow in the winter and spring and declining flow through the summer. Fluctuations of both simulated ground-water levels and discharges are less extreme than those observed, mainly because of the timing, volume, and distribution of recharge. Error in estimating the lateral distribution of hydraulic conductivity and specific yield would also cause simulated values to deviate from observed values.

Discrepancies between computed and observed discharge can be partly explained by error in the recharge specified in the model; other sources of error could be seasonal factors that affect drain conductance, such as (1) the lengthening of drainage channels during wet periods, and (2) reduced permeability of the interface between aquifer and drain surface during dry periods.

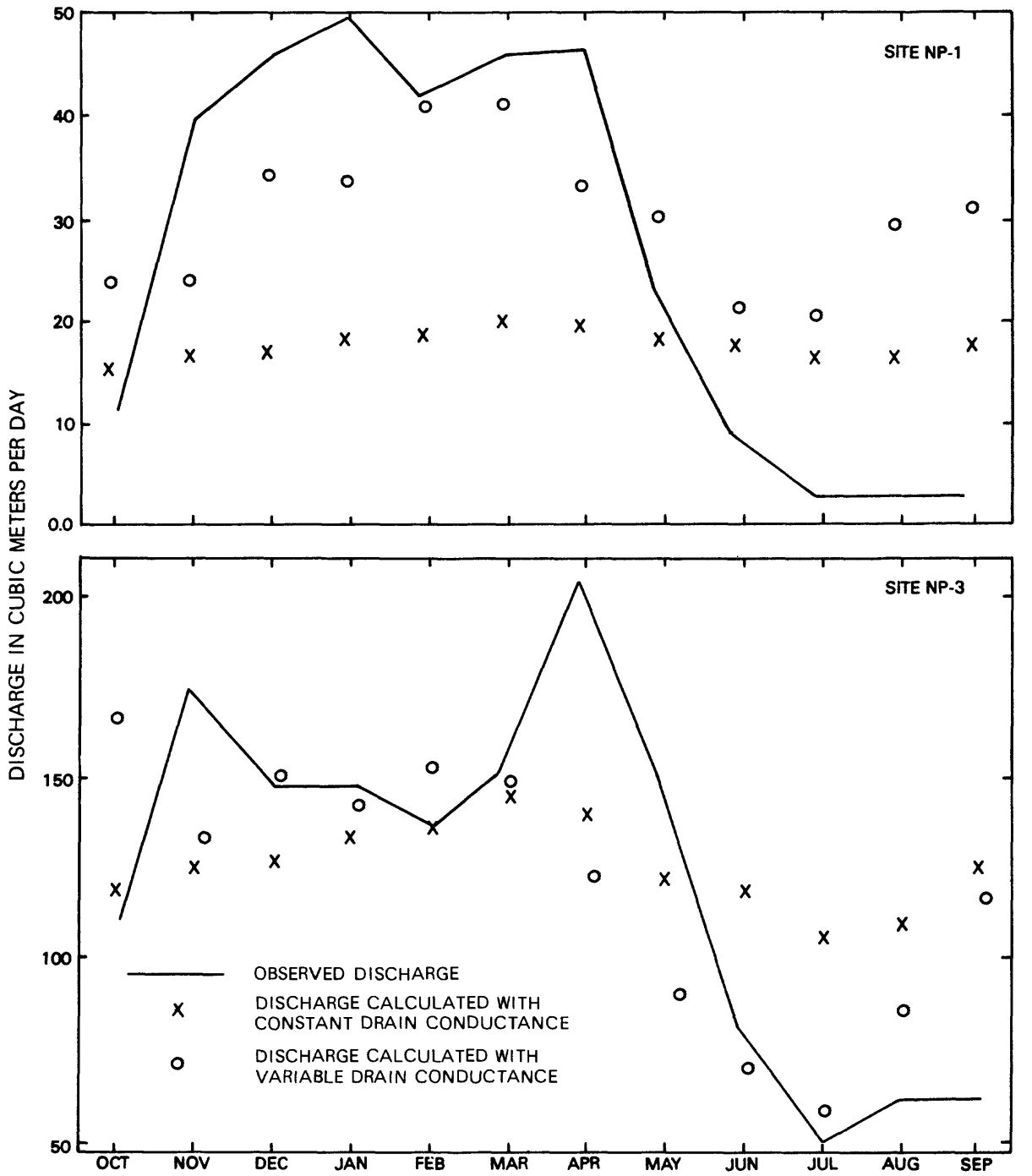

Figure 24.--Measured ground-water discharges at sites NP-1 and NP-3 in relation to discharges simulated from constant and variable drain-conductance values.

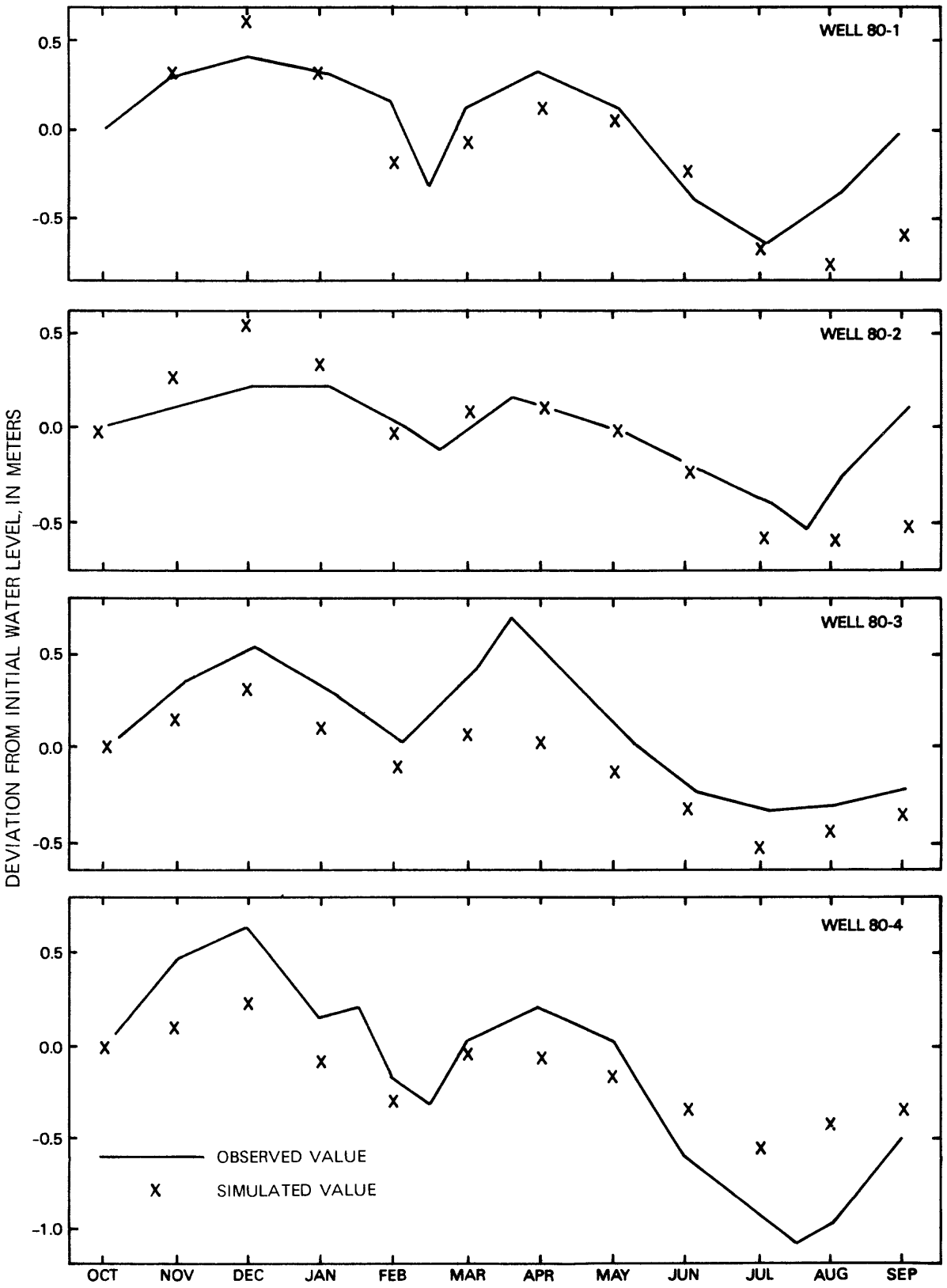

Figure 25.--Measured and simulated water levels

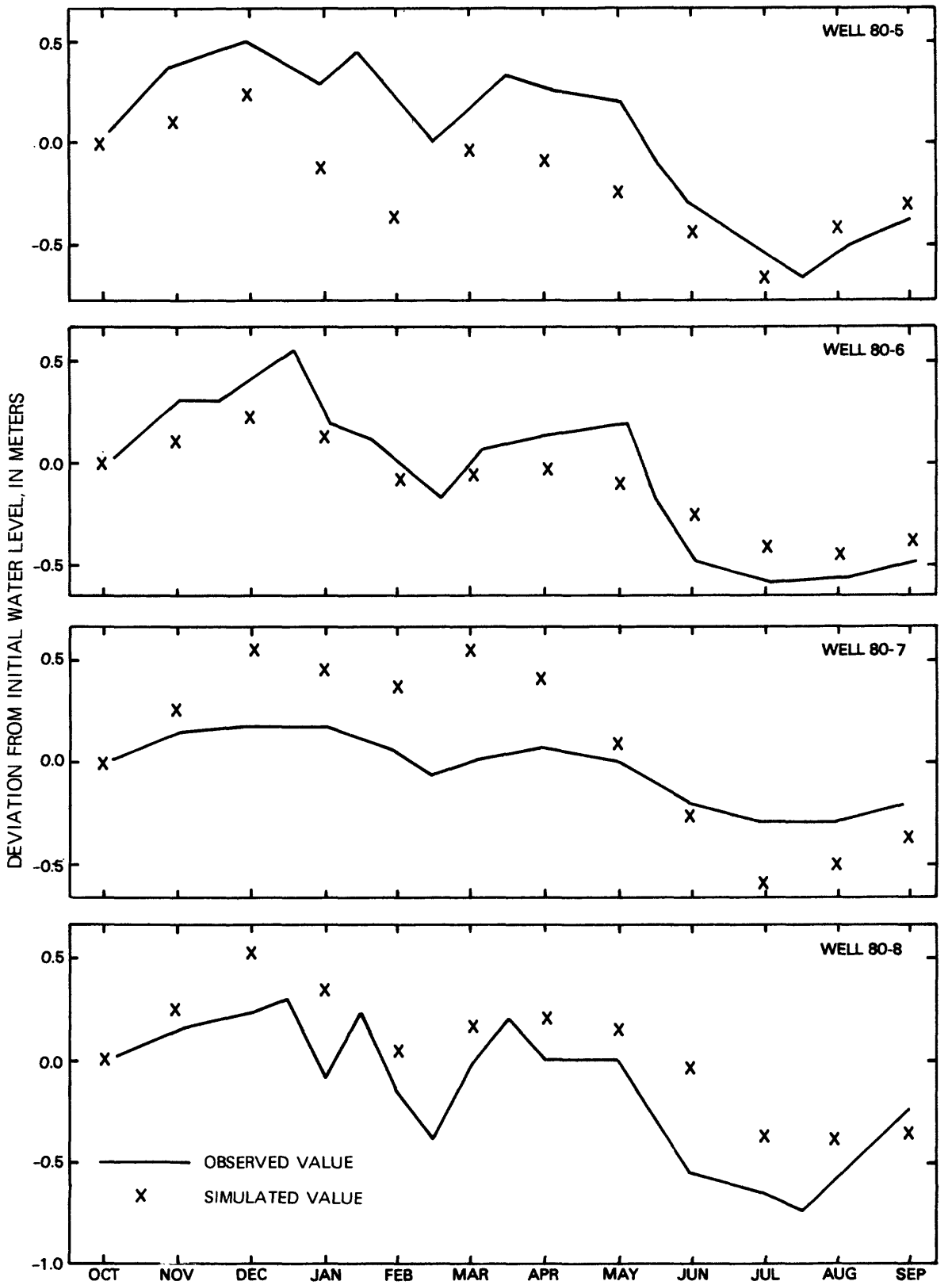

in eight wells. (Well locations are shown on pl. 1.)

MODEL APPLICATION

Tritiated water could infiltrate into the surficial sand and gravel on the north plateau from leaking storage facilities or accidental spills during transport of liquid materials. The ground-water flow model can be used to predict the flow path and velocity of this water, although it neglects the effects of radioactive decay and of mixing during transport. Steady-state simulations calculated flow paths and traveltimes of water from two potential sources of tritium in the reprocessing facility--the main plant building, including the fuel-storage pool, and the high-level liquid-waste-tank complex. Past migration of tritiated water from the low-level waste-treatment system was also simulated, and the results were compared with tritium concentrations measured in 1974.

Ground-Water Movement

Ground-water flow paths and velocities were calculated from the volumetric flux across cell boundaries computed by the steady-state model for each grid cell. The volumetric flux is related to the average linear velocity, V (m/d), by:

$$\overline{V} = \frac{\overline{Q}}{nA} \qquad (8)$$

where: $\overline{Q}$ = volumetric flux, m^3/d,
n = porosity of the saturated material, dimensionless, and
A = average cross-sectional flow area, m^2.

$\overline{V}$ is defined as the ratio between the traveled distance of a ground-water tracer and its time of travel (Freeze and Cherry, 1979, p. 79). The average cross-sectional flow area of a grid cell in the model was assumed to be the product of the saturated thickness of the cell and the grid spacing. The porosity of the surficial gravel was assumed equal to values of specific yield obtained in transient-state simulations. The average linear velocity calculated for each grid cell was plotted as a vector to indicate the rate and direction of ground-water flow.

Ground-water flow paths through the north plateau as predicted by the steady-state model are plotted in figure 26. Most of the ground water entering the north plateau through the upland (southwestern) boundary is diverted by building foundations and backfill associated with the main plant facility to seepage faces above the tributary to Franks Creek. Ground water flowing through the northwestern part of the plateau discharges to the NP-1 channel and the wetland above the NP-3 channel.

Predicted ground-water flow paths from the main plant to discharge points along the east boundary of the plateau are shown in figure 27, which also indicates traveltimes from the fuel-storage pool and the high-level liquid-waste-tank complex to discharge points. The final destination of a slug of water traveling through the surficial sand and gravel will depend upon where it is introduced. The model predicted that the NP-3 channel and the french drain will intercept most of the flow downgradient from these two potential sources and that the remainder will be discharged at seepage faces along the east boundary of the plateau. Water from the main plant area would reach the NP-3 channel and french drain within 500 days and would arrive at the seepage

faces within 800 days. The area of high permeability northeast of the main plant building (fig. 11) significantly decreased the traveltime of water flowing to the NP-3 channel.

Doubling the model hydraulic conductivity did not significantly alter these traveltime predictions, mainly because it created a lower hydraulic gradient in the area of higher permeability, which leaves the ground-water velocity unchanged. Decreasing hydraulic conductivity by 50 percent increased traveltimes from the main-plant area to the NP-3 channel from 500 days to 800 days.

Analysis of Past Tritium Migration

Before the detection of tritium in ground water in 1972, lagoons 4 and 5 were leaking, and the channel above station NP-3 had not been constructed. These conditions were incorporated into the model by draining the model wetland through the former channel above station NP-2 and simulating infiltration from the lagoons as leakage through a confining layer. The amount of leakage predicted by the model was 0.6 L/s, or nearly 50 percent of the total estimated volume of wastewater processed (P. Burn, West Valley Nuclear Service Center, oral commun., 1984). Although this leakage value is unrealistically large, it represents a "worst case" from which to interpret model results.

Steady-state ground-water flow paths in 1972 were predicted from the optimum hydraulic values shown in table 4. Because annual precipitation in 1972 (117 cm) was greater than the annual rate of 92 cm/yr used to estimate recharge for the steady-state calibration, it is likely that the recharge rate in 1972 was also greater than assumed. The increased recharge in steady-state simulations did not have a significant effect on ground-water flow paths through the north plateau, however.

The 1972 ground-water flow paths predicted by steady-state simulation are plotted in figure 28 with tritium concentrations in ground-water samples collected in 1974. The flow lines indicate that leakage from lagoons 1, 4, and 5 moves to the french drain and seepage faces along the eastern boundary of the plateau and do not indicate migration of tritium from lagoons 4 and 5 to the wetland, even at the higher simulated rate of leakage.

Tritium data from 1978 (fig. 6) indicate that tritium levels in ground water west of lagoons 4 and 5 and in the wetland declined after lagoons 4 and 5 were sealed in 1972. If this decline was caused by the sealing of the lagoons, some mechanism such as dispersion or flow through a buried conduit is needed to explain the lateral migration across the prevailing hydraulic gradient. However, tritium concentrations between the hardstand and the main plant building remained elevated in 1978, which suggests other sources. The measured water levels (fig. 10) and estimated distribution of hydraulic conductivity (fig. 11) indicate that most of the ground water discharging to the wetland would follow the buried channel on the till surface northward from the reprocessing plant. Reprocessing activities were halted in 1972; thus, the tritium sources responsible for contamination of the wetland could have been along this flow path and removed since then, which would explain the general decline in tritium concentrations. The potential sources mentioned earlier--storage of tritiated material on the hardstand, leakage beneath the reprocessing plant, and fallout from the ventilation stack, are likely sources of the tritium in the wetland.

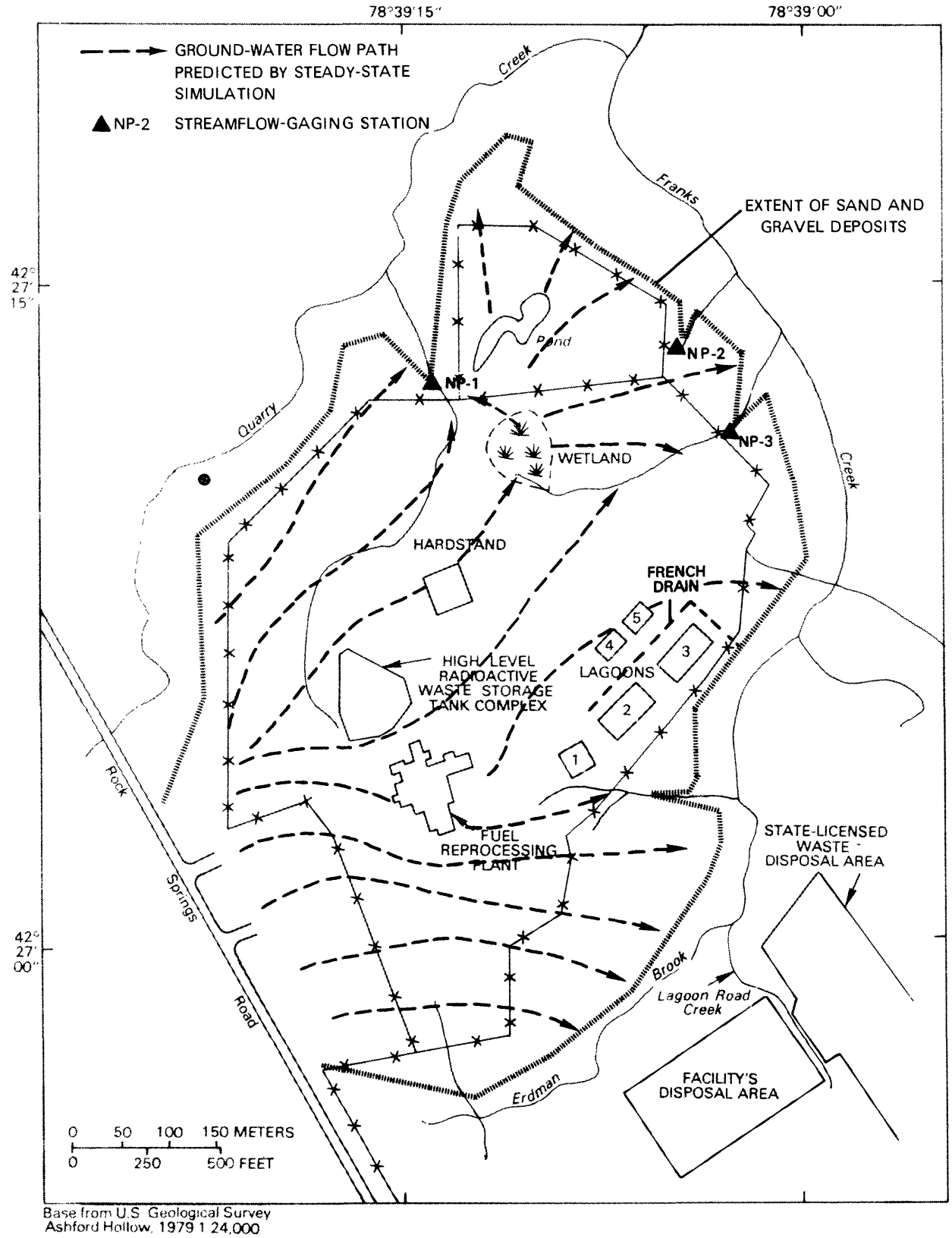

Figure 26.--Ground-water flow paths through sand and gravel on north plateau as predicted by steady-state model.

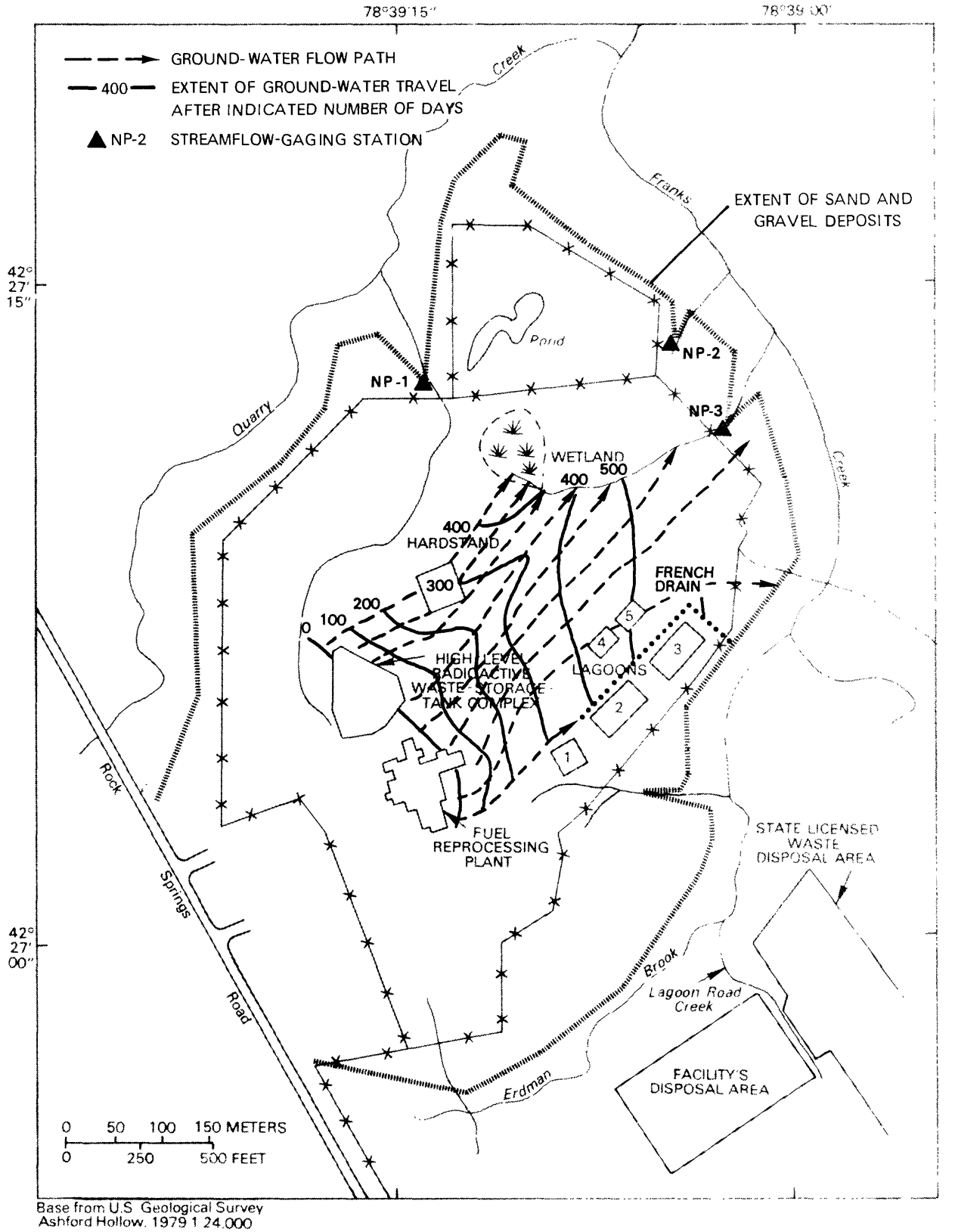

Figure 27.--Flow paths and traveltimes of water from two potential sources of tritium and contamination as predicted by steady-state model.

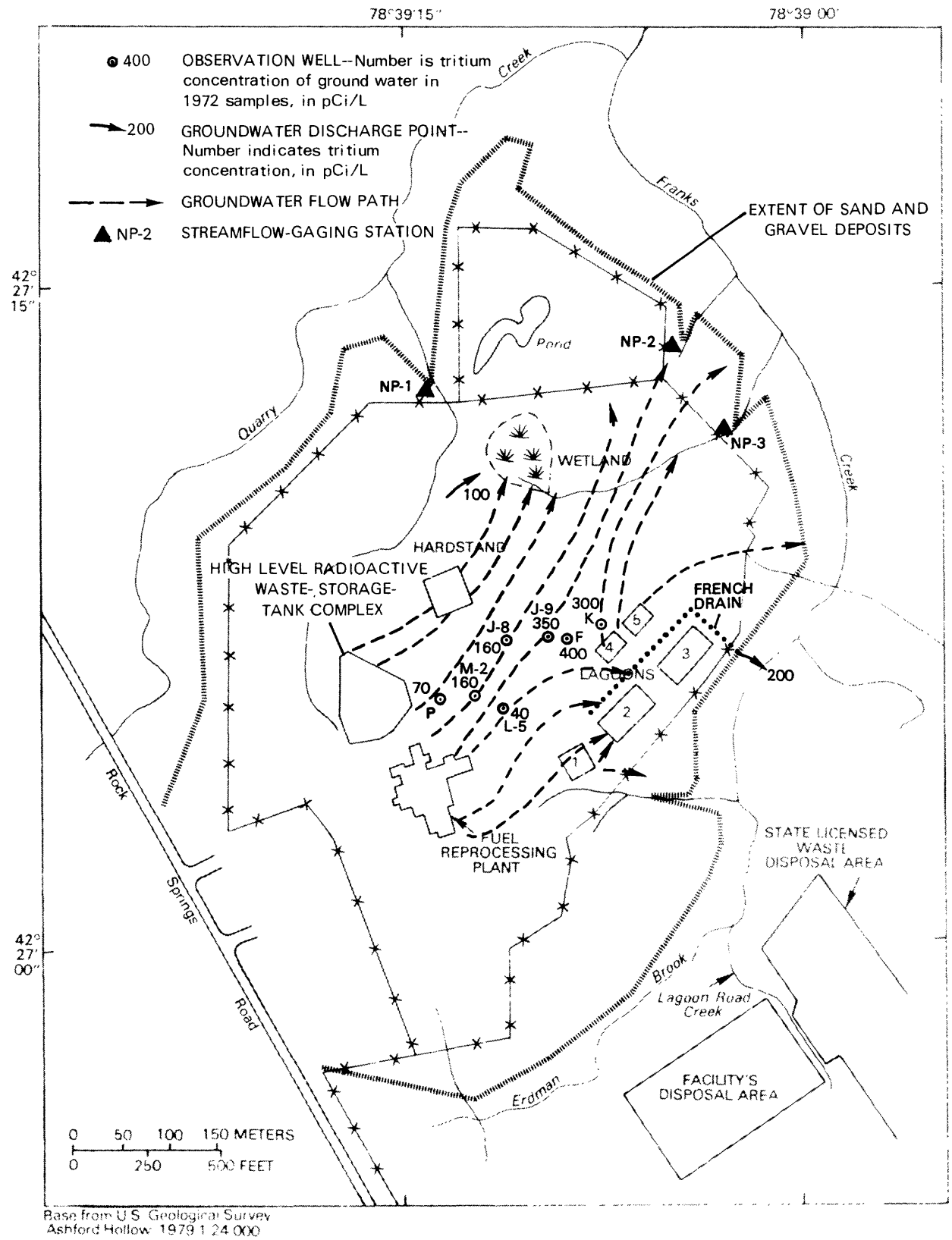

Figure 28.--1972 ground-water flow paths simulated by steady-state model and tritium concentrations in ground-water samples collected in 1974.

SUMMARY AND CONCLUSIONS

A 3-year study was conducted from 1980 through 1983 at the Western New York Nuclear Service Center near West Valley, N.Y., to investigate the hydrogeology and ground-water flow near the former nuclear-fuel-reprocessing plant and its facilities. Radioactive materials are stored within the reprocessing plant and in burial grounds at the site. Tritiated water is stored in a lagoon system near the plant and released under permit to a nearby stream channel.

A two-dimensional finite-difference model was developed to simulate ground-water flow in the surficial sand and gravel deposit underlying the reprocessing plant. The 41.4-ha deposit overlies a till plateau that abuts an upland area of siltstone and shale on its southwest side and is bounded on the other three sides by deeply incised stream channels. The channels drain to Buttermilk Creek, a tributary of Cattaraugus Creek, which drains to Lake Erie.

The ground-water flow model provides a reasonably accurate simulation of lateral ground-water flow through the surficial sand and gravel on the north plateau. Steady-state simulations closely matched the average of ground-water levels recorded in 23 observation wells and ground-water discharges measured at gaging stations NP-1 and NP-3 and the french drain. Transient-state simulations indicated that the model could reproduce seasonal changes in ground-water levels by having the recharge and evapotranspiration rates varied monthly. Transient-state simulation of ground-water discharges matched observed base-flow hydrographs most closely when the values of drain conductance were varied monthly.

Model-generated ground-water levels and discharges were found to be sensitive to the values of recharge and drain conductance. Error in the calibrated values of these terms would affect the ground-water budget predicted by the model or the simulated volume of ground water flowing through the system. However, model predictions of ground-water flow paths and velocities were relatively insensitive to these terms.

Conclusions from the model analysis can be summarized as follows:

1. Model simulations indicated that most ground water flowing from potential sources of tritium near the main plant building would discharge into the stream channel above station NP-3 or the french drain. Some ground water originating near the main plant would discharge through seepage faces along the southeast border of the plateau.

2. The estimated traveltime of ground water from the main plant building to the closest discharge point, calculated from hydraulic conductivity and porosity (assumed equal to specific yield) values obtained through model calibration, was 500 days. Doubling the hydraulic conductivity did not significantly alter this estimate, but decreasing hydraulic conductivity by 50 percent increased the traveltime to 800 days.

3. The model was used to investigate possible sources of the tritium that was found in the wetland on the north plateau in 1972. Although the tritium levels declined after wastewater lagoons 4 and 5 were sealed in 1974, ground-water flow paths predicted by steady-state simulations did not

indicate the lagoons to be a probable source of the tritium. Possible reasons for the migration of tritium from the lagoons to the wetland could include other transport processes, dispersion, or buried conduits. Alternatively, the tritium could have infiltrated to the wetland from other sources.

4. Calibrated model values of hydraulic conductivity of the surficial sand and gravel ranged from 0.6 to 10.0 m/d. The highest values were applied to an area northeast of the main plant building that overlies a buried stream channel incised in the surface of the till. This high permeability significantly decreased traveltime of ground water from the main plant building to the NP-3 channel.

5. More than 75 percent of the ground water on the north plateau (46 cm/yr) is derived from precipitation. Underflow from the fractured bedrock along the upland (south) boundary of the plateau and leakage from the outfall channel from the main plant building into the sand and gravel account for the remainder. Evapotranspiration from the North Plateau totals about 20 cm/yr. Ground-water discharge through seepage faces along the periphery of the plateau totals 3.0 L/s, and discharge to the NP-3 channel totals 1.3 L/s. Discharges to the NP-1 channel, the french drain, and the low-level radioactive wastewater-treatment system account for the remaining 0.8 L/s.

REFERENCES CITED

Albanese, J. R., Anderson, S. L., Dunne, L. A., and Weir, B. A., 1983, Geologic and hydrologic research at the Western New York Nuclear Service Center, West Valley, New York, in U.S. Nuclear Regulatory Commission, Annual Report, August 1981-July 1982: NUREG/CR-3207, 397 p.

Bergeron, M. P., 1985, Records of wells, test borings, and geologic sections near West Valley, New York: U.S. Geological Survey Open-File Report 83-682, 95 p.

Bergeron, M. P. and Bugliosi, E. F., Ground-water flow near two radioactive-waste disposal areas at the Western New York Nuclear Service Center, Cattaraugus County, New York--results of flow simulation: U.S. Geological Survey Water-Resources Investigations Report 86-4351 (in press).

Bergeron, M. P., Kappel, W. M., and Yager, R. M., 1987, Geohydrologic conditions at the nuclear-fuels reprocessing plant and waste-management facilities at the Western New York Nuclear Service Center, Cattaraugus County, New York: U.S. Geological Survey Water-Resources Investigations Report 85-4145, 49 p.

Cooper, H. H., Jr., Bredehoeft, J. D., and Papadopulos, S. S., 1967, Response of a finite-diameter well to an instantaneous charge of water: Water Resources Research, v. 3, p. 262-269.

Draper, N. R., and Smith, H. H., 1981, Applied regression analysis, 2nd ed.: New York, John Wiley, 709 p.

REFERENCES CITED (Continued)

Freeze, R. A., and Cherry, J. A., 1979, Groundwater: Englewood Cliffs, N.J., Prentice-Hall, Inc., 604 p.

Gray, D. M., 1970, Principles of hydrology: Canadian National Committee for the International Hydrological Decade, Ottawa, Canada, 635 p.

Kappel, W. M. and Harding, W. E., 1987, Surface-water hydrology of the Western New York Nuclear Service Center, Cattaraugus County, New York: U.S. Geological Survey Water-Resources Investigations Report 85-4309, 36 p.

LaFleur, R. G., 1979, Glacial geology and stratigraphy of western New York Nuclear Service Center and vicinity, Cattaraugus and Erie Counties, New York: U.S. Geological Survey Open-File Report 79-989, 17 p.

McDonald, M. G., and Harbaugh, A. W., 1984, A modular three-dimensional finite-difference ground-water flow model: U.S. Geological Survey Open-File Report 83-875, 528 p.

New York State Department of Environmental Conservation, 1975, Annual report of environmental radiation in New York: Albany, N.Y., 51 p.

Prudic, D. E., 1981, Computer simulation of ground-water flow at a commercial radioactive-waste landfill near West Valley, Cattaraugus County, N.Y., in Little, C. A., and Stratton, L. E., (eds.), Modeling and low-level waste management--an interagency workshop: Oak Ridge, Tenn., Oak Ridge National Laboratory, ORO821, p. 215-248.

_____ 1986, Ground-water hydrologic and subsurface migration of radionuclides at a commercial radioactive-waste burial site, West Valley, Cattaraugus County, New York: U.S. Geological Survey Professional Paper 1325, 83 p.

Steenhuis, T. S., Muck, R. E., and Walter, M. F., 1983, Prediction of water budgets with or without a hardpan, in Proceedings from Conference on advances in infiltration: American Society of Agricultural Engineers, monograph series, December 1983, p. 1-13.

Todd, D. K., 1980, Ground-water hydrology: New York, John Wiley, 535 p.

U.S. Department of Energy, 1979, Western New York Nuclear Service Center Study: Companion Report TID-28905-2, 500 p.

Velleman, P. F., and Hoaglin, D.C., 1981, Applications, basics, and computing of exploratory data analysis: Boston, Mass., Duxbury Press, 354 p.

Winter, T. C., 1981, Uncertainties in estimating the water balance of lakes: Water Resources Bulletin, v. 17, no. 1, p. 82-115.

APPENDIX

ESTIMATION OF HYDRAULIC CONDUCTIVITY

Estimates of hydraulic conductivity of the surficial sand and gravel were derived by applying the method of Cooper and others (1967) to the results of slug tests done at eight observation wells. The application of the Cooper method is described in Bergeron and others (1987), and values of hydraulic conductivity obtained from the slug-test data are summarized in table A-1. The Cooper method assumes that an instantaneous slug of water is added to a well that fully penetrates a confined, water-bearing layer and that the flow from the well is therefore horizontal with no vertical component.

The geometric mean hydraulic-conductivity value of 0.6 m/d given in table A-1 served only as a starting point in the development of the model because these assumptions were not fully met on the north plateau. First, ground water in the sand and gravel is unconfined; thus the saturated thickness near the well changed during slug tests, which gave rise to vertical flow components. The assumptions were more valid for wells in which the saturated thickness was large relative to the initial increase in water level, whereby the variation in saturated thickness was relatively smaller.

The water level in the well dropped substantially before the first water-level measurement could be made because of the rapid movement of water from the well to the gravel. This problem was partly mitigated by the small diameter (5 cm) of the observation wells, but initial water levels were extrapolated from the data for use by the Cooper method. An error of 25 percent in the initial water-level estimate resulted in an error of more than 40 percent in the calculated hydraulic conductivity.

Table A-1.--Hydraulic-conductivity values for sand and gravel on the north plateau as determined from slug-test data by the method of Cooper and others (1967).

[Well locations are shown on pl. 1.]

Well number	Hydraulic conductivity (m/d)	Saturated thickness (m)	Initial increase in water level (m)
80-1	2.5	4.5	1.0
80-2	.2	2.5	1.1
80-3	7.9	1.0	0.7
80-4	.2	1.6	1.2
80-5	.2	3.3	1.1
80-6	.1	.8	1.7
80-7	.4	.6	1.2
80-8	1.5	2.8	2.0
Geometric mean	0.6		

The lateral variation in hydraulic conductivity of the surficial sand and gravel was investigated at 24 observation wells that had been previously installed on the north plateau for ground-water sampling. These wells were constructed with 15-cm-diameter perforated pipe, so rapid losses of water to the unsaturated zone during a slug test precluded the application of the method of Cooper and others (1967) to determine hydraulic conductivity. Therefore, relative estimates of hydraulic conductivity were calculated from pumping and slug-test data from these wells.

Data on well yields were obtained from records of the previous site operator. The yields were calculated from the maximum discharge that could be derived from the wells after 30 minutes of pumping. These data (table A-2) were normalized by dividing the yield by the saturated thickness recorded at each well. During slug tests performed in this study, 80 liters of water were introduced into each well, and the rise in water level was measured after 30 seconds. (These data are also listed in table 3.) Regression analysis of the normalized yield in relation to water-level rise indicated an inverse linear relationship between the two variables ($F = 17.6$ at the 90-percent confidence interval; the slope of the line was significantly different from zero). However, the regression equation was a poor predictor of the variance of normalized yield ($r^2 < 0.5$; less than 50 percent of variance was explained by regression) (Draper and Smith, 1981, p. 32).

Examination of the surface elevation of the upper till unit near the main plant building (fig. A-1) indicates that a buried stream channel underlies part of the sand and gravel where many of the sampling wells are located. The channel may be an erosional feature that marks the location of a former stream channel cut into the surface of the till plateau. To test the hypothesis that the buried channel may affect the hydraulic conductivity at the wells, the data in table 7 were subjected to a box-plot analysis. Box-plot analysis is a nonparametric statistical technique used to determine whether groups of data are significantly different from each other (Velleman and Hoaglin, 1981, p. 65).

Results of a box-plot analysis are given in figure A-2, which uses three hydraulic-conductivity categories from table A-2 to group the data. The plots indicate that the distribution of data from wells over the buried channel (group 2) is significantly different from that for wells south of the channel (group 1), as evidenced by the lack of overlap in the data. This indicates that the hydraulic conductivity of the sand and gravel overlying the buried channel is higher than that of the gravel east of the channel at a significance level of 5 percent. The sand and gravel west of the channel (group 3) is also significantly different from the other two areas and has an intermediate hydraulic conductivity value. These findings were incorporated into the model and are discussed in the section on the results of steady-state simulations.

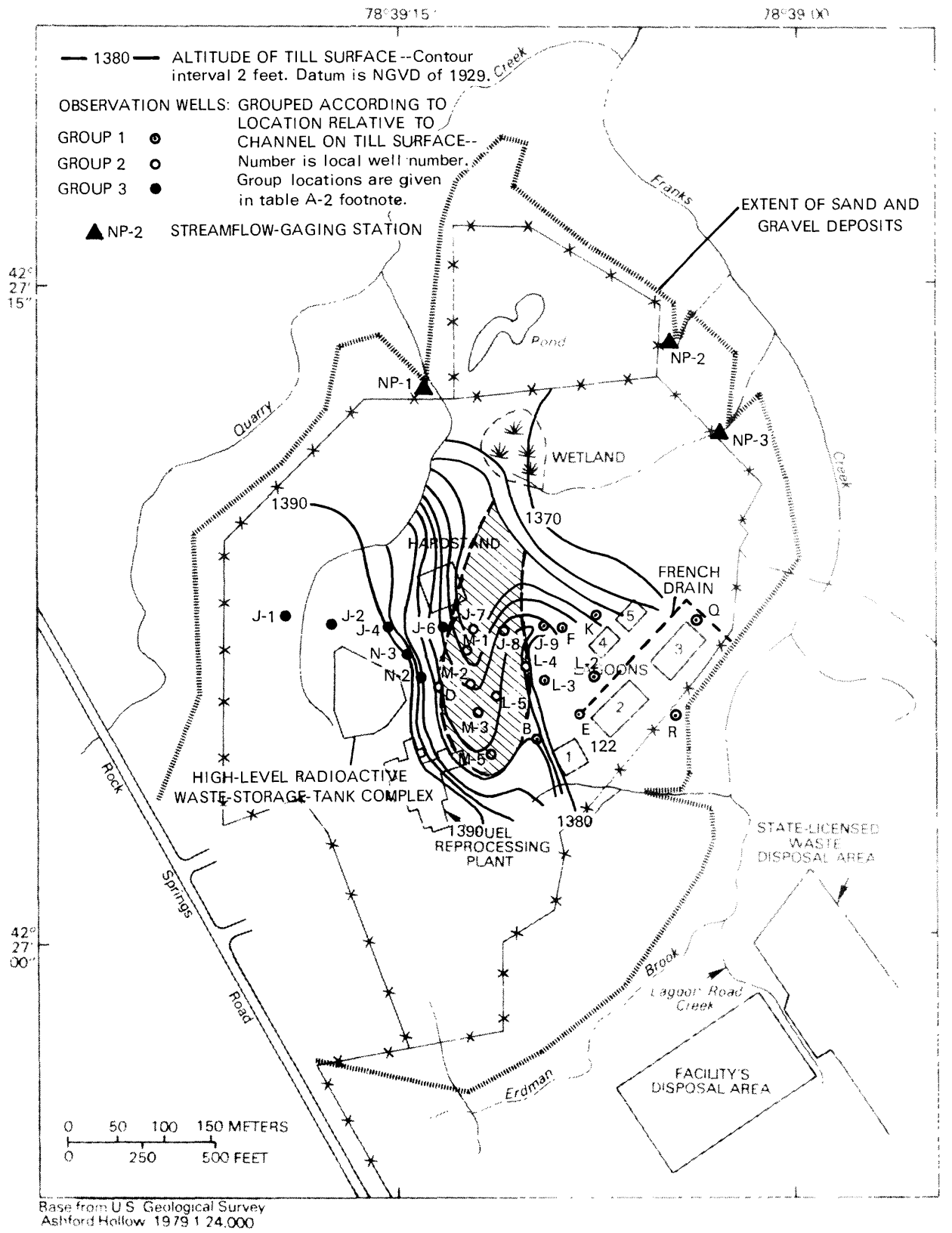

Figure A-1.--Till-surface altitude near main plant and location of buried stream channel.

Table A-2.--Relative measures of hydraulic conductivity developed from pumping and slug-test data from 15-cm-diameter wells.

[Locations of wells and buried channel are shown in fig. A-1.]

Well	Well yield normalized by saturated thickness (L/s)/m	Water-level rise 30 seconds after addition of 30 liters of water (m)	Hydraulic conductivity group used in statistical analysis[1]
B	<.002	1.32	1
E	.004	2.01	1
F	.010	1.50	1
J-1	.186	.66	3
J-2	.064	.65	3
J-4	.031	.76	3
J-6	.079	1.15	3
J-7	.052	.73	2
J-8	.110	.44	2
J-9	.103	.81	1
K	.010	1.43	1
L-2	.010	1.40	1
L-3	.010	2.11	1
L-4	>.103	.83	2
L-5	.058	.29	2
M-1	>.145	.79	2
M-2	>.074	.16	2
M-3	>.093	.45	2
M-5	.116	.34	2
N-2	.006	.87	3
N-3	.037	1.64	3
P	.103	.21	2
Q	.103	.73	1
R	.010	1.35	1

[1] Hydraulic-conductivity group

Location	Relative hydraulic conductivity	Number of observations
East of buried channel	Low	9
Over buried channel	High	9
West of buried channel	Intermediate	6

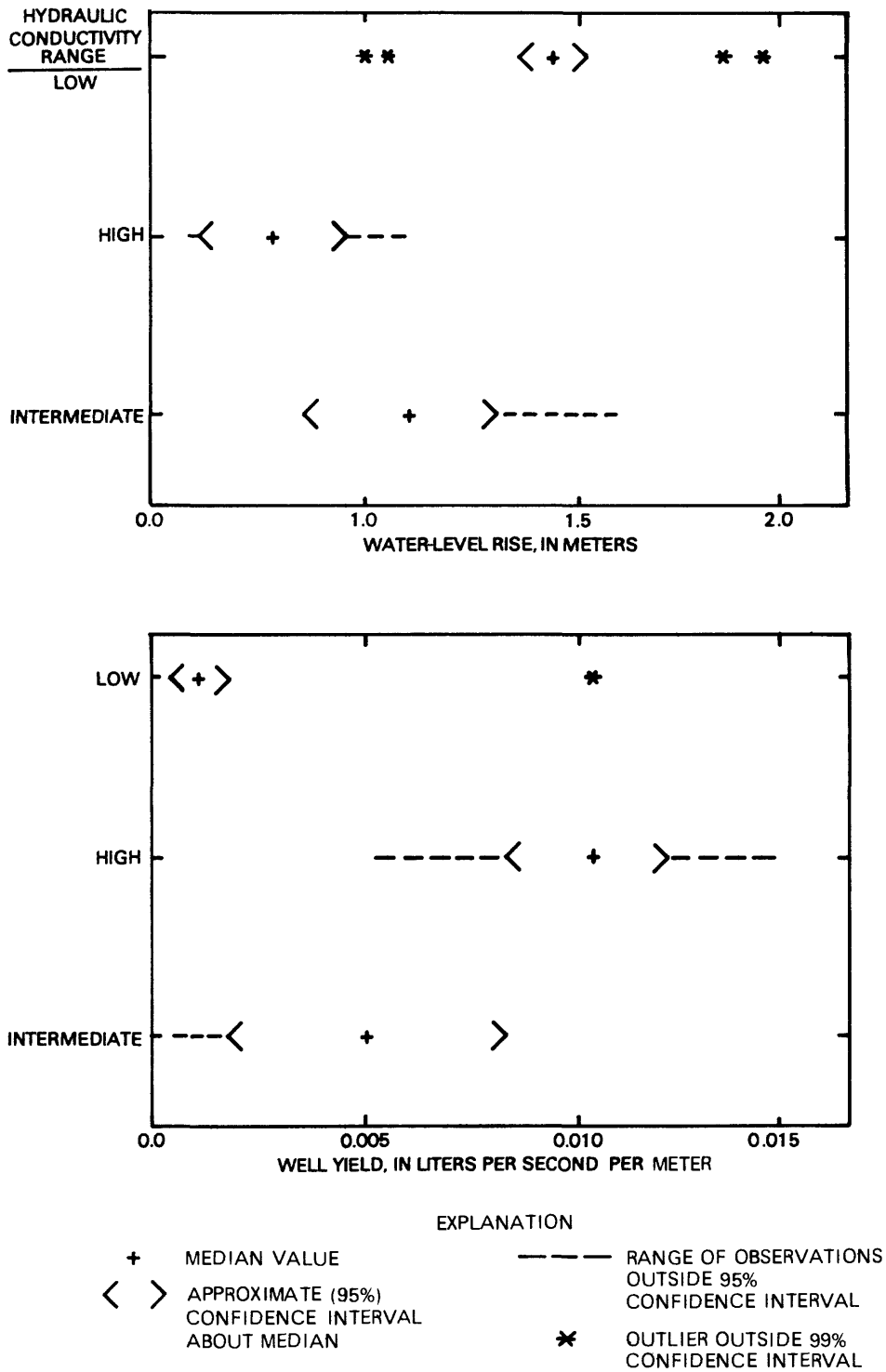

Figure A-2.--Results of box-plot analysis illustrating differences in hydraulic conductivity at observation wells grouped as high, medium, or low according to their location in relation to the buried channel.

☆ U.S. GOVERNMENT PRINTING OFFICE: 1987-712-715